



High Frequency, Short Bunch Width, Slow Extraction for KOPIO

Shane Koscielniak

Abstract

Slow extraction from a synchrotron refers to the deliberate (but weak) excitation of a betatron resonance so that transverse oscillation amplitudes, of charged particles, cross into the acceptance of an extraction septum. We consider the case of a $1/3$ integer resonance driven by sextapole magnets; and an extreme form of chromatic extraction known as *micro-bunching*. This technique will be employed, at the BNL AGS, in the search for the CP violating decay $K_L \rightarrow \pi^0 \nu \bar{\nu}$. To facilitate this, the Slow Extracted Beam (SEB) must be chopped with 250 ps bursts every 40 ns. Based on the simulation of a variety of SEB schemes, we identify factors which promote short extracted bunch width and their influence on resonance crossing and septum hits.

Contents

1	Slow Extraction	3
2	SEB simulation program	3
2.1	Summary of physics	3
2.2	Chromatic effects	4
3	Appropriate separatrix?	4
3.1	Resonance width	5
3.2	AGS SEB parameters	5
4	Micro-bunching	6
4.1	Simulation artefact	6
5	Brief summary of results	7
5.1	25 MHz fundamental; $h = 67$	7
5.2	93 MHz fundamental; $h = 251$	7
5.3	Figure conventions	7
6	Factors influencing microbunch extraction	8
6.1	Central momentum of bucket	8
6.2	Septum hits	8
6.3	Resonance crossing	9
6.4	Chromaticity	10
6.5	Higher harmonics	10
6.6	Inter-bunch extinction	11
6.6.1	Main magnet ripple	11
6.6.2	Orbit bump ripple	12
6.7	Collective effects	12
6.7.1	New simulation algorithms?	12
7	Conclusion	12
7.1	Comments	14
7.2	Acknowledgements	14
8	Simulations Gallery	14
8.1	apr05,apr06,apr08; $\xi = -15.7$, 25 MHz	15
8.2	may25,may26,apr10,may28,apr11; $\xi = -15.7$, dual harmonic	16
8.3	may30,apr25,apr23; $\xi = -31.5$, dual harmonic	18
8.4	may01,may02; $\xi = -31.5$, 93 MHz	19
8.5	may03,may06; $\xi = -15.7$, 93 MHz, $\varepsilon_H = 100\pi\mu\text{m}$	20
8.6	may22,18,21,23,16,24,19,17; $\xi = -15.7$, 93 MHz, $\varepsilon_H = 10\pi\mu\text{m}$	21
9	Output from SLEXPLOT	23

10 Tables	30
10.1 Explanation of symbols	30
10.2 Summary of results; 25MHz	31
10.3 Summary of results; 93MHz	32

List of Figures

1	Variation of betatron tune with amplitude for a variety of bare tunes.	5
2	Phase space during (-8ms) and after (0.0ms) 50 kHz/s bucket sweep; 25may01	6
3	Variation of microbunch width and phase versus frequency offset	9
4	phase space (95ms) and micro-bunch, 05apr, $\Delta p/p\% = 0.46$; $\sigma_\phi = 3$ ns . . .	15
5	phase space (95ms) and micro-bunch, 06apr, $\Delta p/p\% = 0.53$; $\sigma_\phi = 0.67$ ns . .	15
6	phase space (200ms) and micro-bunch, 08apr, $\Delta p/p\% = 0.60$; $\sigma_\phi = 1.36$ ns .	15
7	phase space (190ms) and micro-bunch, 25may, $\Delta p/p\% = 0.46$; $\sigma_\phi = 1.4$ ns .	16
8	phase space (215ms) and micro-bunch, 26may, $\Delta p/p\% = 0.50$; $\sigma_\phi = 0.67$ ns .	16
9	phase space (200ms) and micro-bunch, 10apr, $\Delta p/p\% = 0.53$; $\sigma_\phi = 0.37$ ns .	16
10	phase space (315ms) and micro-bunch, 28may, $\Delta p/p\% = 0.56$; $\sigma_\phi = 0.64$ ns .	17
11	phase space (300ms) and micro-bunch, 11apr, $\Delta p/p\% = 0.60$; $\sigma_\phi = 0.74$ ns .	17
12	phase space (200ms) and micro-bunch, 30may, $\Delta p/p\% = 0.23$; $\sigma_\phi = 0.77$ ns .	18
13	phase space (400ms) and micro-bunch, 25apr, $\Delta p/p\% = 0.265$; $\sigma_\phi = 0.2$ ns .	18
14	phase space (400ms) and micro-bunch, 23apr, $\Delta p/p\% = 0.30$; $\sigma_\phi = 0.44$ ns .	18
15	phase space (600ms) and micro-bunch, 01may, $\Delta p/p\% = 0.26$; $\sigma_\phi = 0.23$ ns .	19
16	phase space (300ms) and micro-bunch, 02may, $\Delta p/p\% = 0.26$; $\sigma_\phi = 0.2$ ns .	19
17	phase space (700ms) and micro-bunch, 03may, $\Delta p/p\% = 0.53$; $\sigma_\phi = 0.42$ ns .	20
18	phase space (1100ms) and micro-bunch, 06may, $\Delta p/p\% = 0.60$; $\sigma_\phi = 1$ ns . .	20
19	phase space (500ms) and micro-bunch, 22may, $\Delta p/p\% = 0.46$; $\sigma_\phi = 1.24$ ns .	21
20	phase space (300ms) and micro-bunch, 18may, $\Delta p/p\% = 0.49$; $\sigma_\phi = 1.8$ ns .	21
21	phase space (400ms) and micro-bunch, 21may, $\Delta p/p\% = 0.51$; $\sigma_\phi = 1.4$ ns .	21
22	phase space (400ms) and micro-bunch, 23may, $\Delta p/p\% = 0.52$; $\sigma_\phi = 0.74$ ns .	22
23	phase space (300ms) and micro-bunch, 16may, $\Delta p/p\% = 0.53$; $\sigma_\phi = 0.44$ ns .	22
24	phase space (400ms) and micro-bunch, 24may, $\Delta p/p\% = 0.54$; $\sigma_\phi = 0.55$ ns .	22
25	phase space (300ms) and micro-bunch, 19may, $\Delta p/p\% = 0.55$; $\sigma_\phi = 0.89$ ns .	23
26	phase space (400ms) and micro-bunch, 17may, $\Delta p/p\% = 0.60$; $\sigma_\phi = 1.69$ ns .	23
27	Output from SLEXPLOT option G: 25apr	24
28	Output from SLEXPLOT option L: 25apr	25
29	Output from SLEXPLOT option T: 25apr	26
30	Output from SLEXPLOT option G: 16may	27
31	Output from SLEXPLOT option L: 16may	28
32	Output from SLEXPLOT option T: 16may	29

1 Slow Extraction

Slow extraction from a synchrotron refers to the deliberate (but weak) excitation of a betatron resonance so that transverse oscillation amplitudes, of charged particles, cross into the acceptance of an extraction septum. When the identity of particles falling on resonance is strongly influenced by their longitudinal momentum, extraction is referred to as *chromatic*. We consider the case of a 1/3 integer resonance driven by sextapole magnets; and an extreme form of chromatic extraction known as *micro-bunching*. In the BNL AGS-2000 era, this technique[1] will be employed in the search for the CP violating decay $K_L \rightarrow \pi^0 \nu \bar{\nu}$ competing with the background $K_L \rightarrow \pi^0 \pi^0$. To facilitate this, the AGS Slow Extracted Beam (SEB) must be chopped with 250 ps bursts every 40 ns.

2 SEB simulation program

SLEX-LONG1D is a Fortran-77 computer program for first order simulation of slow extraction systems employing chromatic 1/3 integer betatron resonance. SLEX is an acronym for SLOW EXtraction. The original SLEX[2] was written by Ulrich Wienands for study of the proposed KAON Factory Extender ring. The present SLEX is documented elsewhere[3].

2.1 Summary of physics

The SLEX-LONG1D simulation is 2+2 dimensional, i.e. the longitudinal motion is treated separately from the radial motion. However, the longitudinal motion feeds into the horizontal motion via the chromatic dependencies of betatron tune, etc. The horizontal motion is derived from the hamiltonian[4]

$$H(Q, P) = \frac{1}{2} \delta \nu_i(t, \Delta p) [Q^2 + P^2] + A(t) [3PQ^2 - P^3]. \quad (1)$$

The coordinates Q, P are taken in a frame rotating with tune $\nu_{res} = m/3$. In this frame, the particles are brought approximately to rest; there is a small residual rotation rate $\delta \nu_i$, and some amplitude growth due to the non-linear drive terms. A is the Fourier component of the sextapole strength around the ring. Let α and β be Courant-Snyder values, and C and S cosines and sines. Q, P are related to the position and divergence x, x' via the transformation (2) which results in an upright triangular separatrix.

$$\begin{bmatrix} Q \\ P \end{bmatrix} = \begin{bmatrix} C & -S \\ +S & C \end{bmatrix} \frac{1}{\sqrt{\beta}} \begin{bmatrix} 1 & 0 \\ \alpha & \beta \end{bmatrix} \begin{bmatrix} x \\ x' \end{bmatrix}. \quad (2)$$

Simulation is done by symplectic numerical integration of the equations of motion:

$$\frac{dQ}{dt} = + \frac{\partial H}{\partial P}, \quad \frac{dP}{dt} = - \frac{\partial H}{\partial Q}. \quad (3)$$

Particles are generated and “tracked” in normalized betatron phase space (Q,P). Extracted particles are transformed back to (x, x') space before analysis of the result.

2.2 Chromatic effects

The individual particle tune is $\nu_i = \nu_{\text{bare}} + \Delta\nu_i$ where the chromatic tune shift is:

$$\Delta\nu_i = \frac{\Delta p_i}{p_0} \left[\xi_1 + \xi_2 \frac{\Delta p_i}{p_0} \right]. \quad (4)$$

The individual tune distance to resonance is $\delta\nu_i = \nu_i - \nu_{\text{res}}$.

- There are offsets to the horizontal position and divergence introduced through the dispersion function.
- There is also chromatic variation of the Courant-Snyder parameters.
- The longitudinal motion is governed by the usual difference equations.

3 Appropriate separatrix?

When extraction is *achromatic*, there is a unique separatrix. Its size depends on the distance between the bare tune and resonant tune, and upon the sextapole strength parameter. In the achromatic case, the spread of betatron tunes depends only upon amplitude; and all trajectories within the separatrix are stable. Typically parameters are adjusted so that, initially, the separatrix just encloses the beam emittance. Then A and/or $(\nu_{\text{bare}} - \nu_{\text{res}})$ are varied to shrink the separatrix and progressively drive particles out.

When extraction is *chromatic*, there is now a spread in the zero-amplitude (i.e. bare) tunes, and one finds a *continuum* of separatrices of different size; one each for every value of $\delta p/p_0$. If the $\delta p/p_0$ spread is large enough some particles will obtain negative tune distances, in which case their individual triangle and sense of rotation become inverted. When extraction is chromatic, whichever single separatrix we choose to plot can be considered only as being “suggestive and for guidance purposes”. The most useful choice is a separatrix with size equal to the beam horizontal emittance. For the given strength parameter, one may calculate the required tune distance ($\delta\nu_w$) and the momentum offset to achieve such a distance between the resonant tune and the zero amplitude tune. This choice of separatrix is useful in that it indicates from what region of the particle distribution are the particles most likely to be extracted.

Figure 1 attempts to clarify this discussion. The figure answers the following type of question: “for a given bare tune difference, what amplitude is required to touch the separatrix?” In other words, when does the amplitude-dependent tune difference fall to zero and lock the motion into resonance? The black curve shows variation of tune with amplitude for trajectories inside some medium-sized separatrix. This nominal $\delta p/p_0 = 0$ separatrix is larger than the beam emittance. The red (upper) and blue (lower) curves show the variation of tune with amplitude for different values of the bare tune. For the blue/red curve the bare tune is closer/further from the resonant tune. The bare tune varies through chromaticity and so blue and red curves relate to off-momentum particles. The blue triangles (at $\pm\delta\nu_w$, etc.) show areas equal to the beam emittance. The beam will occupy some area on figure 1 to the left of the “beam-emittance” vertical line, drawn dashed. In a chromatic extraction scheme, the central momentum changes as a function of time and so the beam-occupied-area

will slowly move downward. When particles move across the area enclosed by the blue curve, they will lock on to resonance and become extracted; this is the separatrix we adopt below.

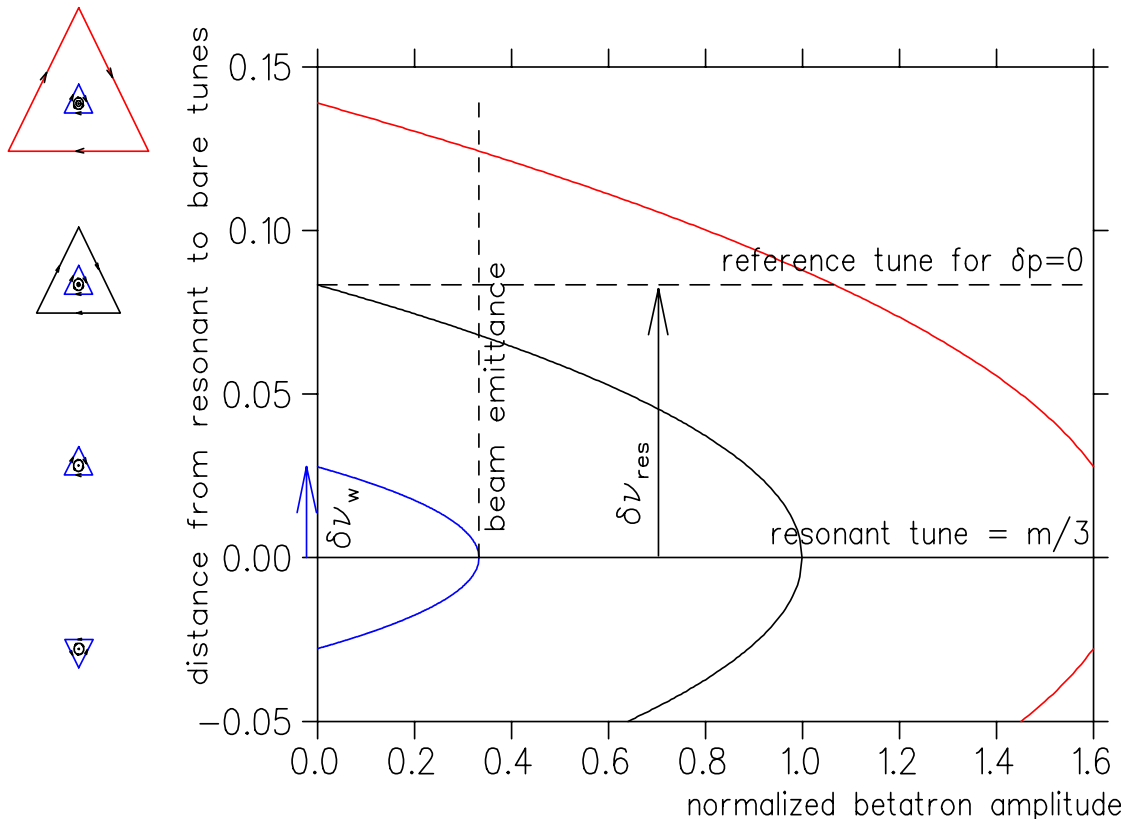


Figure 1: Variation of betatron tune with amplitude for a variety of bare tunes.

3.1 Resonance width

The triangular separatrix with area equal to the transverse emittance ε_H has vertices $[\pm Q_0, -P_0]$ and $[0, +2P_0]$ where $Q_0 = \pm(\pi\varepsilon_H/\sqrt{3})^{1/2}$ and $P_0 = Q_0/\sqrt{3}$. Here we take Q_0 positive (negative) if the nominal tune is above (below) the integral resonance. The $\frac{1}{3}$ integer resonance is unusual in that it has pure real (i.e. not complex) fixed points when approached from either above or below in betatron tune.

- Particles with zero betatron amplitude come into resonance when $\delta\nu_i = 0$.
- Particles with betatron amplitudes touching the emittance boundary come into resonance (i.e. fall on the separatrix) when their bare tunes satisfy $|\delta\nu_i| \leq 6P_0A \equiv \delta\nu_w$. The resonance width in $\Delta p/p$ is $\pm\delta\nu_w/\xi$.

3.2 AGS SEB parameters

For the AGS SEB, the bare tune is $\nu_{\text{bare}} \approx 8.75$ and the $\frac{1}{3}$ -integer resonance occurs at $\nu_{\text{res}} = 8.6667$. For particles with zero betatron amplitude, the resonance centre occurs at a $\Delta p/p$ offset of 0.529% when chromaticity $\xi = -15.7$, and at $\Delta p/p = 0.264\%$ when chromaticity $\xi = -31.5$.

4 Micro-bunching

In the micro-bunching scheme, the beam is unbunched and the r.f. cavity is neither accelerating nor decelerating. However, the guide magnetic field is changing and so, at constant momentum, the beam moves radially – outward if the field falls. Relative to the synchronous momentum (for the magnet field) the beam appears to accelerate. In the simplest scenario, the r.f. tracks the synchronous revolution frequency but with a constant offset. Hence the empty r.f. bucket appears as a barrier to movement in the (longitudinal) momentum direction; and the small gap between neighbour buckets acts as a venturi through which particles may pass. If this venturi is made to coincide with the $\Delta p/p$ width of the betatron resonance, then extracted particles comprise of a (very) small r.f. phase width.

It has to be realised that the “venturi” is a projection of a 4-dimensional extraction volume and this has two consequences: (i) particles exit not just from the narrowest part of the $\phi, \Delta p$ constriction, but from a range of Δp ; and (ii) that extraction is transverse and so few (ideally zero) pass through the $\phi, \Delta p$ constriction.

In the AGS it is intended to achieve synchronous phase values (radian) of a few parts in 10^4 . The venturi is some 10^{-2} radian at its narrowest; but the Δp width of the resonance will broaden the microbunch phase-width.

4.1 Simulation artefact

In later figures, you will see fine structure in the phase space of the extracted micro-bunches; you are forewarned that this is mostly an artefact.

In the AGS proton beams are accelerated from 1.5 GeV to 24 GeV before extraction. Ideally the micro-bunching cavities are energised, at the extraction r.f., well in advance of extraction so that the beam adapts adiabatically to the quasi-coasting phase space structure they will impose. This ideal, and realisable, practise is not simulated. Instead, empty r.f. buckets are swept into a 24 GeV coasting beam in a non-adiabatic fashion, and this introduces substantial fine structure into the phase space occupied by the particle ensemble; figure 2 shows an example of this. The effect, which is transmitted to the microbunches, is made more acute by the fact that only the upper $\frac{1}{3}$ of the beam in $\Delta p/p$ is tracked in the interest of computational expediency.

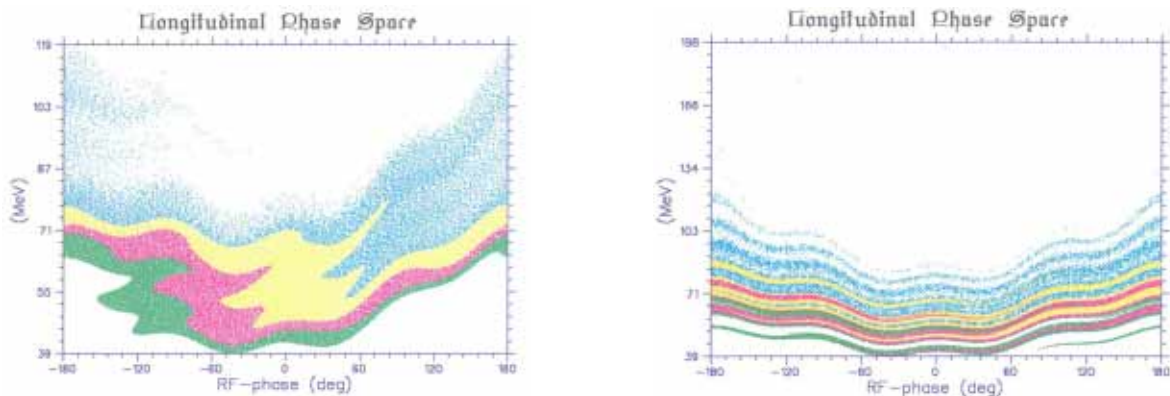


Figure 2: Phase space during (-8ms) and after (0.0ms) 50 kHz/s bucket sweep; 25may01

5 Brief summary of results

The symbols appearing in the tables are defined in section 10.1

5.1 25 MHz fundamental; $h = 67$

Case name	$-\dot{B} \times 10^3$ (T/s)	$-\xi$ #	V_1 (kV)	V_4 (kV)	$\Delta p/p$ %	A 10^{-3}	$\delta p/p$ 10^{-4}	σ_ϕ (ns)	95% (ns)	hits %	cross %	$\bar{\phi}_{ac}$ (deg)	Fig. #
05apr	7.727	15.7	100	–	0.46	1.0	4.41	2.97	14.2	8.1	1.01	32.3	4
06apr	7.727	15.7	100	–	0.53	1.0	3.45	0.67	2.65	2.9	1.70	3.96	5
08apr	7.727	15.7	100	–	0.598	1.0	2.86	1.36	5.82	4.5	0.187	-7.91	6
25may	2.576	15.7	150	150	0.460	1.25	6.44	1.40	6.05	4.1	0.7	11.1	7
26may	2.576	15.7	150	150	0.495	1.25	6.00	0.669	3.24	3.0	0.9	2.93	8
10apr	2.576	15.7	150	150	0.53	1.2	3.80	0.371	1.47	1.8	3.64	-2.65	9
28may	2.576	15.7	150	150	.5635	1.25	3.43	0.637	2.728	1.2	0.76	-6.13	10
11apr	2.576	15.7	150	150	0.598	1.3	3.64	0.743	3.34	1.0	0.219	-7.47	11
30may	1.288	31.5	150	150	0.230	1.0	2.95	0.771	3.217	5.1	7?	5.30	12
25apr	1.288	31.5	150	150	0.264	1.0	1.79	0.200	0.80	4.1	7.0?	-0.85	13
23apr	1.288	31.5	150	150	0.299	1.0	1.63	0.438	1.94	1.5	1.8?	-3.37	14

Normalized emittance is $\varepsilon_H = 100 \pi \mu\text{m.radian}$.

5.2 93 MHz fundamental; $h = 251$

Case name	$-\dot{B} \times 10^3$ (T/s)	$-\xi$ #	V_4 (kV)	ε_H $\pi \mu\text{m}$	$\Delta p/p$ %	A 10^{-3}	$\delta p/p$ 10^{-4}	σ_ϕ (ns)	95% (ns)	hits %	cross %	$\bar{\phi}_{ac}$ (deg)	Fig. #
01may	1.288	31.5	20	100	0.264	1.0	1.63	0.233	0.992	1.3	0.848	-6.51	15
02may	1.288	31.5	100	100	0.264	1.0	1.52	0.196	0.784	1.2	2.00	-6.62	16
03may	2.576	15.7	20	100	0.53	1.4	4.10	0.424	1.783	1.1	.096	-18.5	17
06may	2.576	15.7	20	100	0.598	1.4	3.95	1.042	4.40	1.0	.0074	-53.1	18
22may	2.576	15.7	20	10	0.460	1.4	1.26	1.24	5.36	2.9	0.258	-125.	19
18may	2.576	15.7	20	10	0.492	1.4	1.79	1.848	7.4	8.9	0.305	137.	20
21may	2.576	15.7	20	10	0.508	1.4	2.49	1.395	6.60	4.6	0.6	48.7	21
23may	2.576	15.7	20	10	0.518	1.4	1.95	0.740	3.50	4.1	1.17	15.1	22
16may	2.576	15.7	20	10	0.53	1.4	1.54	0.438	1.76	3.6	3.4	-7.88	23
24may	2.576	15.7	20	10	0.540	1.4	1.38	0.549	2.62	3.2	1.5	-23.9	24
19may	2.576	15.7	20	10	0.550	1.4	2.00	0.89	3.76	3.2	0.79	-37.8	25
17may	2.576	15.7	20	10	0.598	1.4	1.46	1.69	6.8	2.9	0.268	-77.8	26

5.3 Figure conventions

We apologise that picture quality was sacrificed in favour of small file size. The upper and lower branches of the longitudinal separatrix are shown yellow and green, respectively. The betatron resonance centre line is shown blue, and the resonance width is indicated by the brown/coral lines above and below. It helps in understanding these figures to appreciate that particles with positive $\Delta p/p$ move from right to left.

6 Factors influencing microbunch extraction

6.1 Central momentum of bucket

The betatron resonance is located at $\Delta p_{\text{res}}/p_s = (\nu_{\text{bare}} - \nu_{\text{res}})/\xi$. Where should one place the central momentum of the rf bucket? Figures 4 through 6 show the effect of scanning the bucket across the resonance window in $\Delta p/p$ for the single harmonic case, while figures 7 through 11 show results of a similar scan for dual harmonic r.f. buckets.

In these examples, where the bucket height is considerably greater than the resonance width, it is clear that making the bucket and resonance centres coincident leads to the shortest microbunches, figures 5 and 9. It is also apparent that there is a strong asymmetry about the optimum, and that placing the bucket central momentum above the centre of the betatron resonance also yields quite short microbunches, figures 6 and 10. However, there are side effects that one must be aware of such as *septum hits* and *resonance crossing* which are discussed below. Figure 12 through 14 show a bucket centre momentum scan for larger $|\xi|$ chromaticity.

When the bucket height is smaller than the betatron resonance width, figures 17 and 18, or comparable with it, figures 19 through 26, then the same general trend applies of minimum microbunch length when momentum-centre of bucket and resonance are coincident. The trend is summarized in figure 3 which shows results of a frequency scan. Note that because the AGS is operated above transition energy, negative/positive frequency differences are associated with positive/negative differences in $(\Delta p - \Delta p_{\text{res}})$.

There are new features when r.f. bucket height and betatron resonance width are comparable. Firstly, the narrowness of the microbunches is not strongly related to the venturi $(\phi, \Delta p)$ width; for example, figure 17. Secondly, when bucket and resonance centres are not coincident, the interbunch extinction does not go to zero and the bunch tails may extend over the complete r.f. period; for example, figures 21 and 25.

6.2 Septum hits

The position and divergence (x, x') of particles at the septum depend on the dispersion functions (η, η') and on the orientation angle of the $\frac{1}{3}$ -integer separatrix. This angle reverses sign for negative tune-distances to resonance. The precise momentum bite of extracted particles depends on the location of the bucket, and the corresponding ranges of tune-distances to resonance vary both in magnitude and sign, and may even be bi-polar. Thus the range of divergence angles raining on the septum is influenced, strongly so when one realises that the separatrix is inverted for negative tune distances. This effect accounts for the 4% difference in *septum hits* between the cases depicted in figures 4 and 6. The septum tilt was optimised for the case of *06apr*, figure 5.

Likewise for the cases depicted in figures 7 through 11, the septum hits are fewer when the bucket is centred slightly above the resonance centre even though the septum tilt was optimised on case *10apr*, figure 9.

The same general trend appears in cases *22may* through *17may*, figures 19 to 26. Septum hits are reduced when the bucket centre is placed above the resonance centre because there is little or no possibility for inversion of the separatrix. These cases which have small

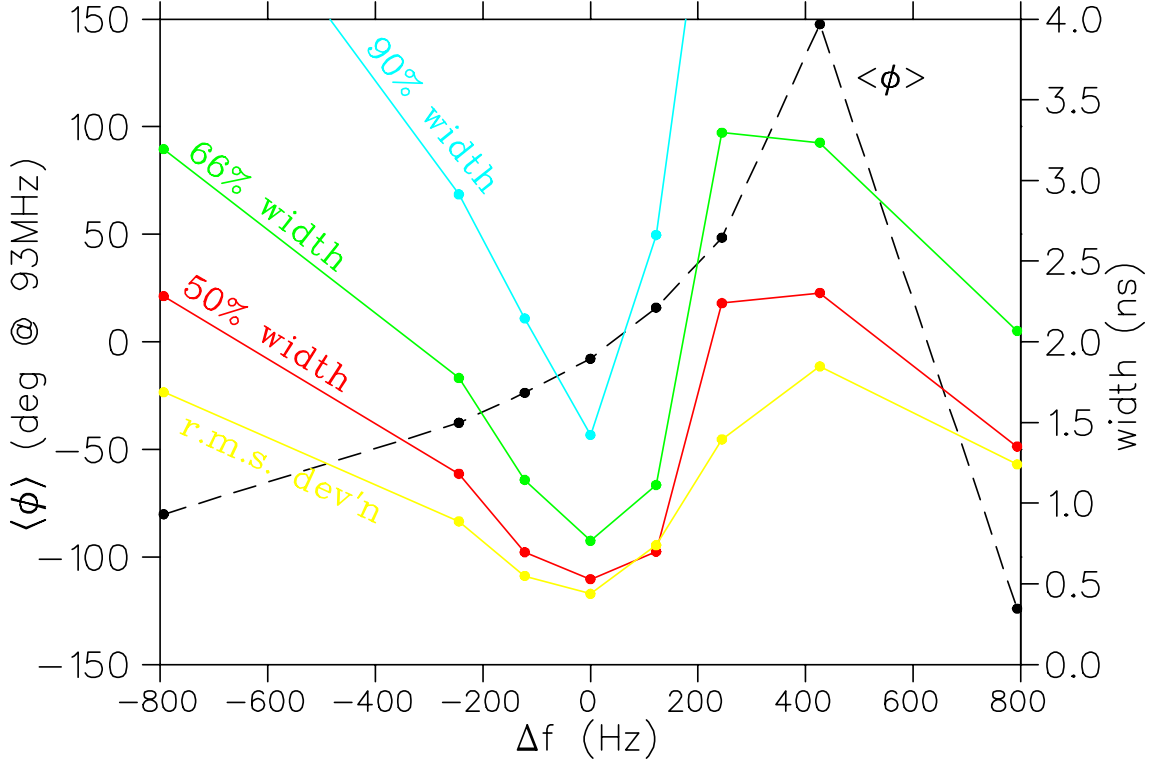


Figure 3: Variation of microbunch width and phase versus frequency offset from beatron resonance for the cases *17may*(-800Hz) through *22may*(+800Hz).

emittance ($\epsilon_H = 10\pi\mu\text{m}$) were not re-optimised and have the same septum tilt angle as case *03may* which was optimised for normalised emittance $\epsilon_H = 100\pi\mu\text{m}$. For the smaller emittance, particles strike only one face of the septum rather than being distributed equally on both faces (which is optimal). The reason for this difference is that the number of pitches along the 1/3-integer separatrix to build up extraction amplitude is different; and results in different density distributions. Compare the transverse characteristics of extracted beams, figures 29 and 32, which originate from different initial circulating emittances of $\epsilon_H = 100\pi\mu\text{m}$ and $\epsilon_H = 10\pi\mu\text{m}$ respectively.

6.3 Resonance crossing

Resonance crossing poses a fundamental limitation to the microbunching extraction scheme. Because of the longitudinal motion the betatron tune varies, carrying the particles toward resonance. Usually in SEB schemes the condition

$$\epsilon_H \times (A^2\pi 6\sqrt{3}) \gg |\xi\Delta\dot{p}/p_s| \quad (5)$$

is satisfied and there is sufficient time for the amplitude to grow large enough for extraction at the septum. However, the gap between neighbour r.f. buckets acts as a venturi; and so the narrower the constriction in rf phase, the faster is the motion in Δp . When it is fast enough, particles may pass through the betatron resonance without being extracted. Such particles are difficult to expel from the machine. They could, perhaps, be ejected after the

extraction spill is completed using either a fast kicker magnet or an a.c. dipole to excite a coherent resonance. [Because the beam is coasting, a kicker would wipe a portion of the beam across the extraction system components.] If such particles are not expelled, they result in increased radio-activation; and if they are expelled they contribute to beam dump handling issues. Consequently, the tolerance for resonance crossing is small. For example, the cases *10apr*, *25apr* and *16may* (figures 9,13,23) result both in the shortest microbunches (for their parameter ranges) and the highest rate of resonance crossing, 3.6%, 7% and 3.4% respectively. Increasing the voltages and/or using yet higher harmonic numbers, cases *29apr* and *26apr* respectively, raises the resonance crossing to unacceptable levels, 14% and 9% respectively. Raising the $|\xi|$ chromaticity modulus will narrow the resonance width and will also promote resonance crossing; for examples cases *30may* through *23apr*, figures 12 to 14.

Crossing also influences septum hits. For example, suppose bucket and resonance centres are coincident. If inequality (5) is satisfied, an upper bound on momentum width of microbunches is $\Delta p_w/p_s = \delta\nu_w/\xi$. If condition (5) is contradicted, the momentum width may rise to $2\Delta p_w$; and sign reversal of $\delta\nu_i$ and the 1/3-integer separatrix will lead to increased septum hits unless the dispersion and separatrix orientation are both zero.

6.4 Chromaticity

The larger the modulus of chromaticity, the smaller is the momentum width of the betatron resonance; which is immediately beneficial to bunch length. Obviously, the resonance central $\Delta p/p$ also changes. The smaller momentum range also implies that the magnet field ramp required to sweep the entire beam across the resonance is smaller. The lowering of $|dB/dt|$ reduces the synchronous phase and narrows the gaps between rf buckets, which is also beneficial. It may be necessary to reduce the momentum width of the initial circulating beam to access these advantages. Contrarily, the narrowing of the venturi also promotes resonance crossing.

One may examine the pairs of cases *03may,01may* (figs. 17,15) and *25may,30may* (figs. 7,12) and *10apr,25apr* (figs. 9,13) and *11apr,23apr* (figs. 11,14) which compare corrected ($\xi = -15.7$) and natural ($\xi = -31.5$) chromaticity to see the narrowing effect on bunch length and increased resonance crossing at larger $|\xi|$. In principle, the narrower resonance width in $\Delta p/p$, at larger $|\xi|$, could result in reduced septum hits; but this would require re-optimisation of the septum tilt angle, etc., and this was not done.

6.5 Higher harmonics

A cavity with an even harmonic antiphased to the fundamental may be used to distort and stretch the r.f. buckets so as to further shorten the bunches. This is more effective than additional voltage at the fundamental¹ for a variety of reasons. The gap between buckets is more responsive to the gradient $dV/d\phi$ of the waveform at the astable fixed point than to the peak voltage. The bucket height can be reduced and the disturbing non-adiabatic effects of sweeping empty buckets into a coasting beam can be much reduced, since the depth of this

¹For example, cases *01may* and *02may*, raising the voltage by a factor 5 leads only to a factor 1.2 reduction in microbunch length; figures 15 and 16.

effect depends on the peak voltage. Evidently, an ideal solution would implement a “barrier bucket” due to a waveform that applies impulses at the bucket ends.

However, with equal 1st and 4th harmonic a more complex longitudinal phase space emerges with 4 fixed points; and the configuration of flow lines becomes complicated when buckets accelerate more strongly. For example, one may get 2 bounding separatrices; one enclosing 3 fixed points and another enclosing 1 fixed point. Such structure can compromise the interbunch extinction; if the initial r.f. sweep is too fast particles may become trapped around inner fixed points and these will experience repeated chances to extract as they rotate about the fixed points. The severity of the effect depends on the ratio of bucket height to resonance width, but a harmonic ratio $|V_4/V_1| = 2$ is probably an upper limit for the AGS parameters.

We refer the reader to the tables in sections 10.2 and 10.3. As anticipated adding another harmonic (2,4, or 6) of equal magnitude (e.g. *11apr*, *17apr*) is more effective than doubling the fundamental voltage, case *18apr*. There are small incremental reductions in microbunch length as the harmonic number is raised. For example, cases *15may*, *10apr* compare 2nd versus 4th harmonic; and cases *25apr2*, *26apr* compare 4th versus 6th harmonic. Because there is an existing design for a 4th harmonic cavity, we concentrated upon that case. Raising the dual harmonic voltage above that of the fundamental also has its advantages and limits. With $V_4/V_1 = -2$, case *29apr*, the shortest microbunches are obtained ($\sigma_\phi = 0.19$ ns) but the crossing rate rises to 14%.

6.6 Inter-bunch extinction

We consider here effects which influence the particle extinction between micro-bunches. The strongest dependence is on the ratio of resonance width to bucket height, and the relative location of their centres; for example, see figures 17 and 18. There are also secondary effects.

The momentum, r.f. phase and betatron amplitude of extracted particles are strongly correlated; the latter 2 may be considered consequences of the former. Thus noise effects which allow particles to cross (diffusively) through the nominal longitudinal separatrix may lead to particle population between the microbunches. Examples of this would be r.f. noise and main magnet ripple; the latter is probably the more severe effect in the AGS.

6.6.1 Main magnet ripple

The present SLEX model has options for single frequency ripple and noise like parts. However, the true situation is a wide number of line harmonics plus smaller random noise; this could be modelled if there is sufficient interest. Magnet field ripple will also have a strong influence on the length of extracted microbunches because motion in the vicinity of the astable fixed point is particularly influenced by the synchronous phase which is strongly coupled to magnetic field rate of change dB/dt . Perhaps the spill servo loop, which modulates dB/dt to maintain constant extraction flux, should also be modelled.

Main magnet ripple in a combined function machine, or quadrupole ripple in a separated function lattice, will modulate the tune and, in turn, the resonance width. Sextupole ripple will also modulate the resonance; and both these effects may have a minor impact on inter-bunch extinction.

6.6.2 Orbit bump ripple

Ripple on the extraction orbit bump could advance or delay the number of pitches a particle moves along the 1/3 integer extraction separatrix before entering the septum; but this is unlikely to have a strong influence on the tails present in microbunches.

6.7 Collective effects

When large circulating beam current is involved (a spill of $\approx 10^{14}$ protons each 3 s) the micro-bunching scheme has the advantage that the charge density and Fourier components of a coasting beam are an order of magnitude smaller than for bunched beam extraction. Consequently, transverse tune shift and spread, cavity beam-loading and other longitudinal wake-fields are all reduced.

Nevertheless, distortion of the longitudinal potential well could be substantial at 100TP, and could ruin the inverse $\sqrt{\text{voltage}}$ scaling law for the gap width between (single harmonic) r.f. buckets. The precise effect depends on the machine longitudinal impedance, particularly at high frequency because microbunching leads to pronounced cusps in the circulating current density. A measurement of micro-bunch length versus injected intensity could uncover the existence or not of this kind of effect – provided that the injected phase-spaces do not change too much as the intensity is varied.

6.7.1 New simulation algorithms?

There is a long history of artefacts introduced when particle motion is approximated by a discretized time-step algorithm, e.g. the order of operations is important. When should longitudinal impedance effects be added in relation to the time-stepping for the transverse motion? If longitudinal effects are included, should there not be some transverse effect of impedance that must be included to maintain symplecticity? It is uncertainties of that type which has prevented SLEX from being advanced in the direction of collective effects. But if experiments[5] like KOPIO and MECO (muon to electron conversion) proceed, it is an area that must be visited.

7 Conclusion

A variety of AGS SEB schemes for *microbunching* has been simulated with various single and dual harmonic voltages, and various B/dt and chromaticity.

Narrow bunches are promoted by:

- bucket centred on betatron resonance
- bucket height \gg resonance width
- high harmonic r.f.
- large modulus of chromaticity
- small magnet field ramp rate

bucket centred

- Advantages: shortest microbunches
- Dis-advantages:
 - increased resonance crossing
 - more septum hits

Implies that bucket centre should be moved slightly above the resonance so that extraction can benefit from the slower movement in Δp ; this increases extraction probability but increases r.f. phase-extent.

bucket height

- Advantages: improved inter-bunch extinction
- Dis-advantages: resonance crossing possibility

high harmonic

consider “barrier bucket”

- Advantages:
 - lower cavity voltages
 - less disruption from r.f. sweep
- Dis-advantages:
 - increased resonance crossing
 - more complicated r.f. system

large chromaticity

may require smaller momentum spread

- Advantages:
 - slower magnet field ramp
 - fewer septum hits
- Dis-advantages:
 - increased resonance crossing
 - transverse optics impact

As a compromise between conflicting objectives, the presently preferred AGS microbunched SEB scheme uses natural chromaticity, a 3 s magnet ramp, 25 MHz fundamental and 4th harmonic with 150 kV on each cavity yielding microbunches with $\sigma_\phi = 0.2$ ns and 7% resonance crossing.

7.1 Comments

- It is obvious that changing sextapole strength, betatron tune, or chromaticity will alter the resonance width.
- Do not forget that varying the emittance will also change the resonance width.
- Do not forget that changing any of A, ν, ξ, ε will require re-optimisation of the septum tilt angle.
- To make extraction insensitive to $\Delta p/p$ requires the $\frac{1}{3}$ -integer separatrix orientation angle to be zero, in addition to zero betatron dispersion functions.
- A simple plot of the longitudinal separatrix superimposed on the betatron resonance width in $\Delta p/p$ is a good guide to extraction behaviour. This is expected to be true also for minibunch extraction for MIKO.
- Collective effects cannot be ignored at 100TP and simulations models should be modified to reflect this.

7.2 Acknowledgements

The author thanks Kevin Brown, Woody Glenn and Thomas Roser of the Brookhaven Alternating Gradient Synchrotron (AGS) Department for the opportunity to work on the AGS slow extraction scheme for KOPIO and for the many stimulating discussions with these colleagues.

8 Simulations Gallery

See figures 4 through 26 for brief comparison of a wide variety of cases; and figures 27 to 32 for a more detailed comparison of two particular cases.

References

- [1] J.W. Glenn et al: *Microbunching of the AGS SLOW Extracted Beam for a Rare Kaon Decay Search*, IEEE Proc. 2001 Particle Accelerator Conf., Chicago Illinois, June 18-22 2001, pg. 1529.
- [2] U. Wienands & R. Servranckx: *Towards a slow extraction system for the TRIUMF Kaon Factory...* Proc. 1st EPAC, Rome, June 1988, pg. 269.
- [3] S. Koscielniak: *SLEX-LONG1D User's Guide*, TRIUMF Report TRI-DN-01-25.
- [4] K.R. Symon: *Extraction at third-integral resonance*, parts I,II,II; Fermilab Notes FN-130, FN-134, FN-140, April 1968.
- [5] Rare Symmetry Violating Processes (RSVP): <http://www.bnl.gov/rsvp/>

8.1 apr05,apr06,apr08; $\xi = -15.7$, 25 MHz

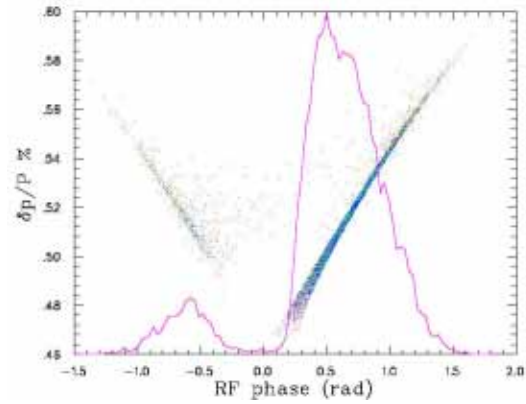
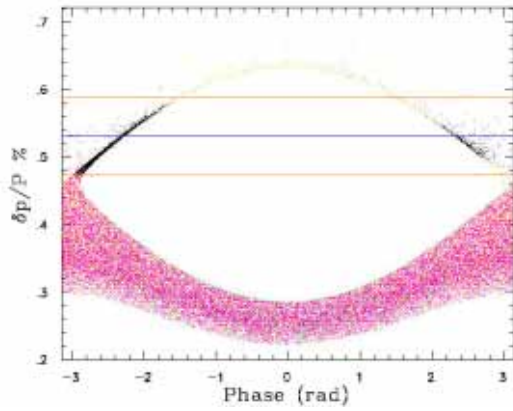


Figure 4: phase space (95ms) and micro-bunch, 05apr, $\Delta p/p\% = 0.46$; $\sigma_\phi = 3$ ns

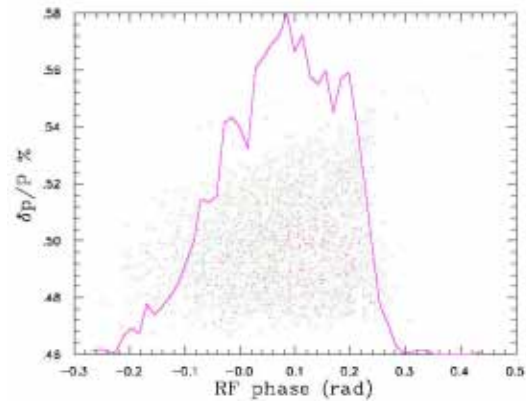
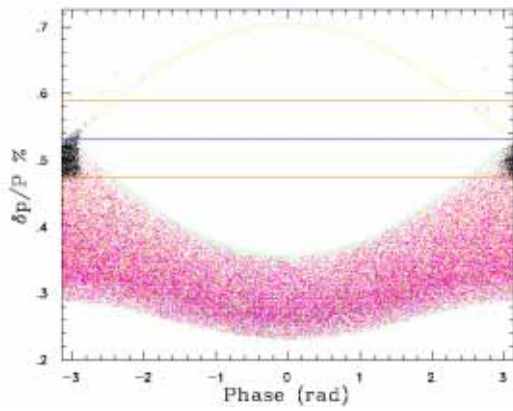


Figure 5: phase space (95ms) and micro-bunch, 06apr, $\Delta p/p\% = 0.53$; $\sigma_\phi = 0.67$ ns

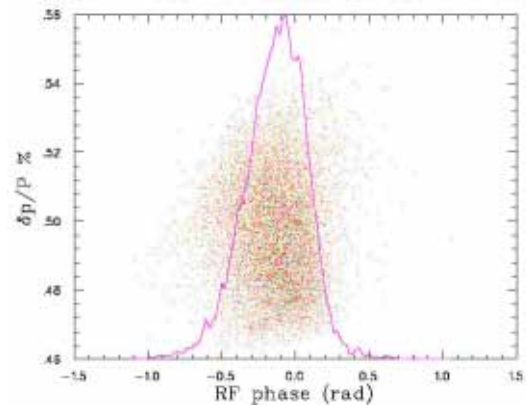
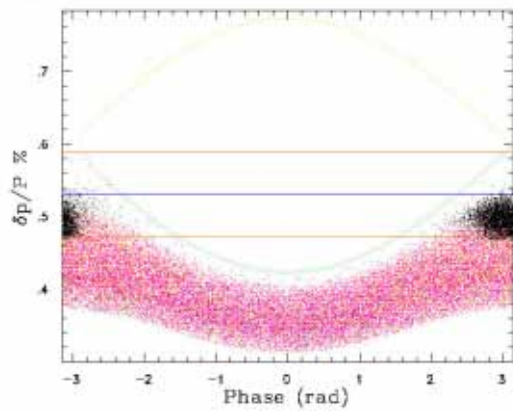


Figure 6: phase space (200ms) and micro-bunch, 08apr, $\Delta p/p\% = 0.60$; $\sigma_\phi = 1.36$ ns

8.2 may25,may26,apr10,may28,apr11; $\xi = -15.7$, dual harmonic

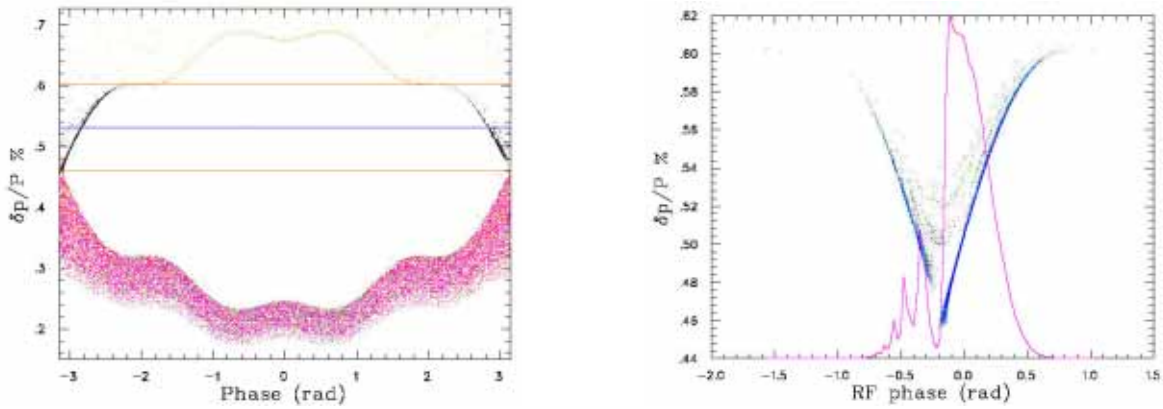


Figure 7: phase space (190ms) and micro-bunch, 25may, $\Delta p/p\% = 0.46$; $\sigma_\phi = 1.4$ ns

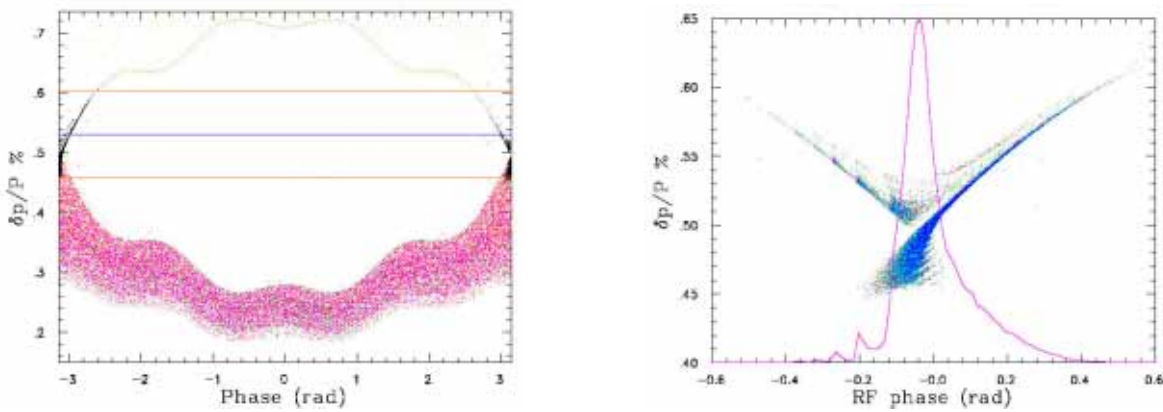


Figure 8: phase space (215ms) and micro-bunch, 26may, $\Delta p/p\% = 0.50$; $\sigma_\phi = 0.67$ ns

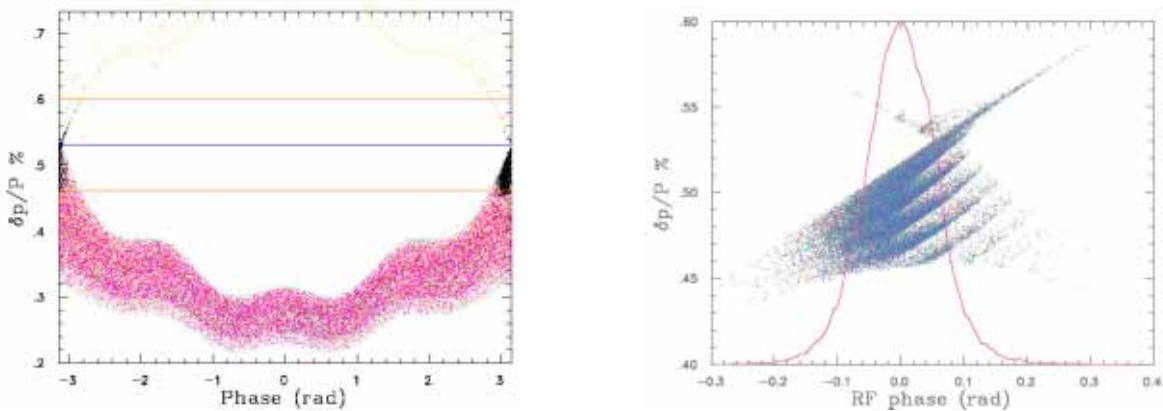


Figure 9: phase space (200ms) and micro-bunch, 10apr, $\Delta p/p\% = 0.53$; $\sigma_\phi = 0.37$ ns

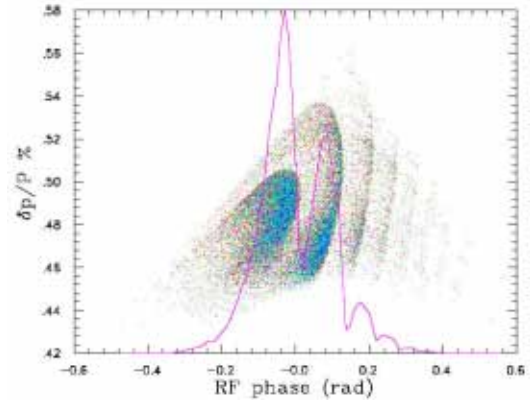
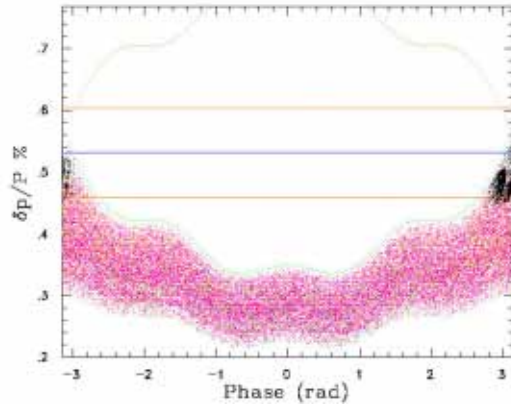


Figure 10: phase space (315ms) and micro-bunch, 28may, $\Delta p/p\% = 0.56$; $\sigma_\phi = 0.64$ ns

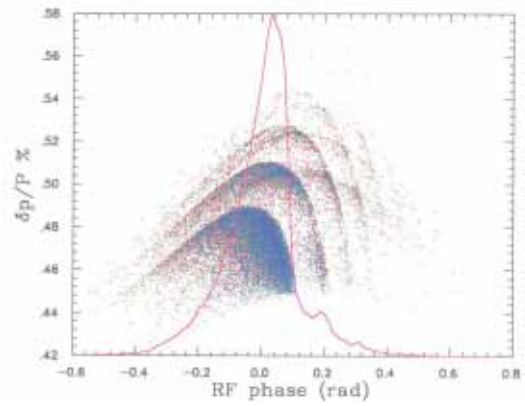
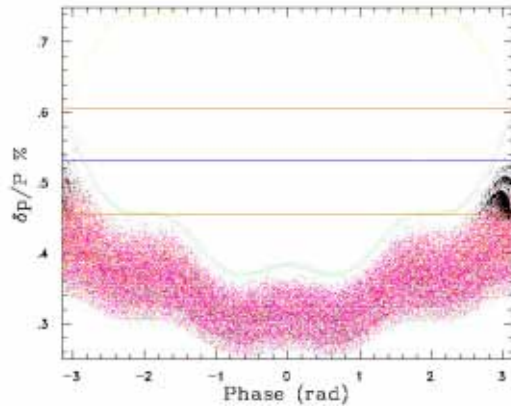


Figure 11: phase space (300ms) and micro-bunch, 11apr, $\Delta p/p\% = 0.60$; $\sigma_\phi = 0.74$ ns

8.3 may30,apr25,apr23; $\xi = -31.5$, dual harmonic

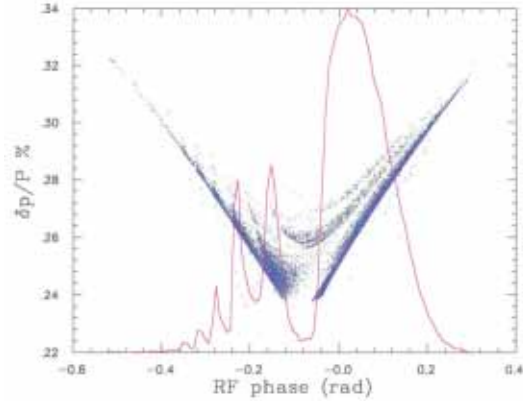
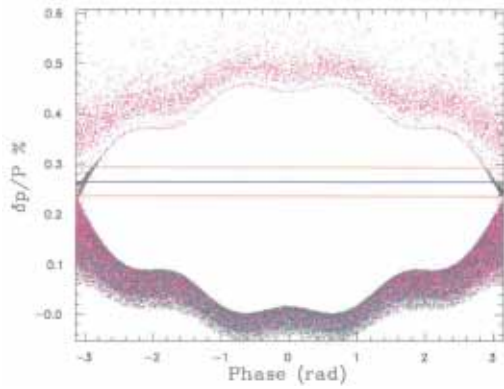


Figure 12: phase space (200ms) and micro-bunch, 30may, $\Delta p/p\% = 0.23$; $\sigma_\phi = 0.77$ ns

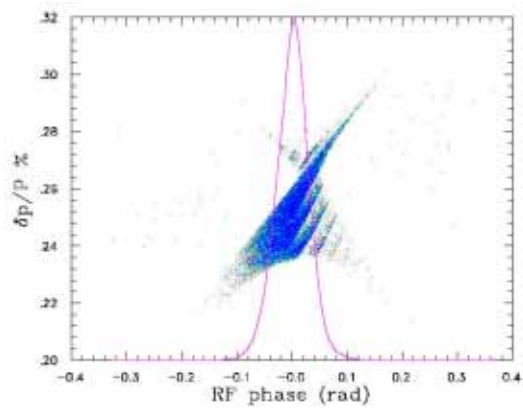
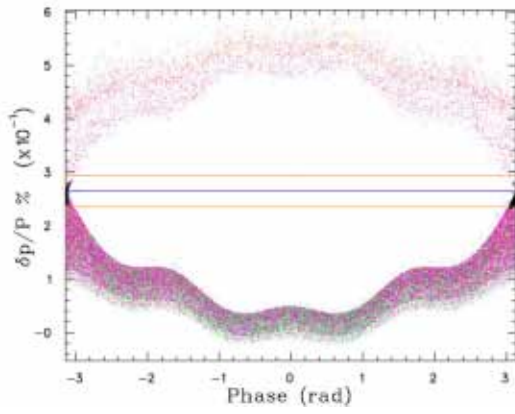


Figure 13: phase space (400ms) and micro-bunch, 25apr, $\Delta p/p\% = 0.265$; $\sigma_\phi = 0.2$ ns

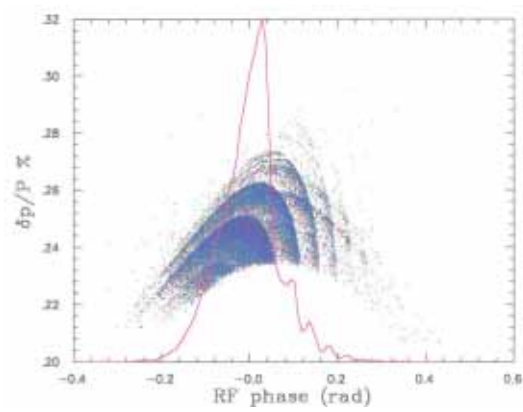
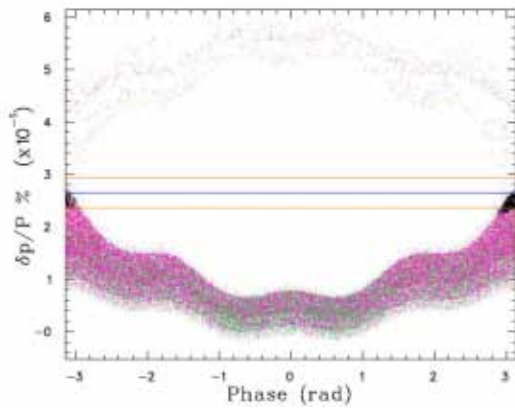


Figure 14: phase space (400ms) and micro-bunch, 23apr, $\Delta p/p\% = 0.30$; $\sigma_\phi = 0.44$ ns

8.4 may01,may02; $\xi = -31.5, 93$ MHz

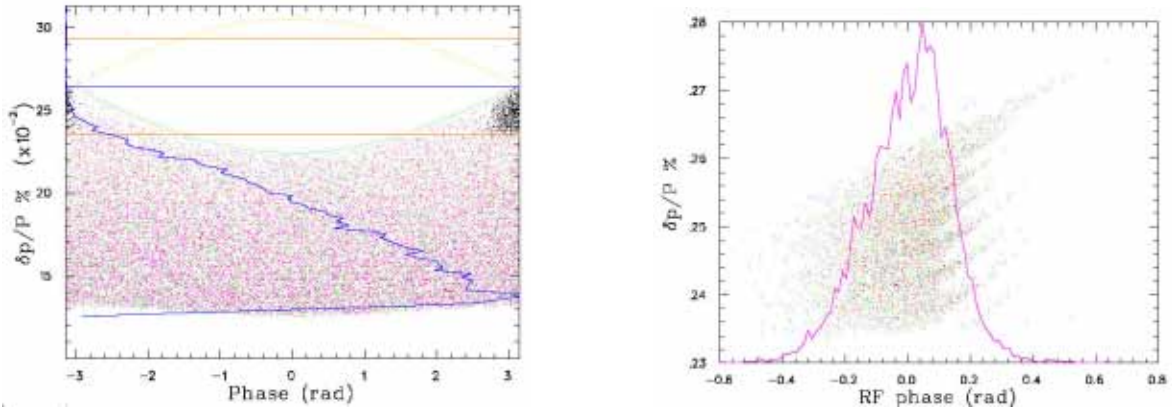


Figure 15: phase space (600ms) and micro-bunch, 01may, $\Delta p/p\% = 0.26$; $\sigma_\phi = 0.23$ ns

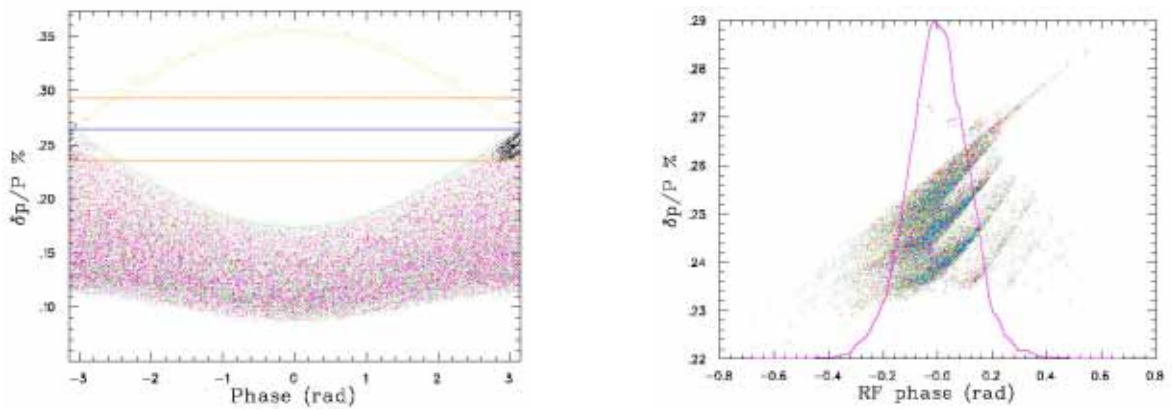


Figure 16: phase space (300ms) and micro-bunch, 02may, $\Delta p/p\% = 0.26$; $\sigma_\phi = 0.2$ ns

8.5 may03,may06; $\xi = -15.7, 93$ MHz, $\varepsilon_H = 100\pi\mu\text{m}$

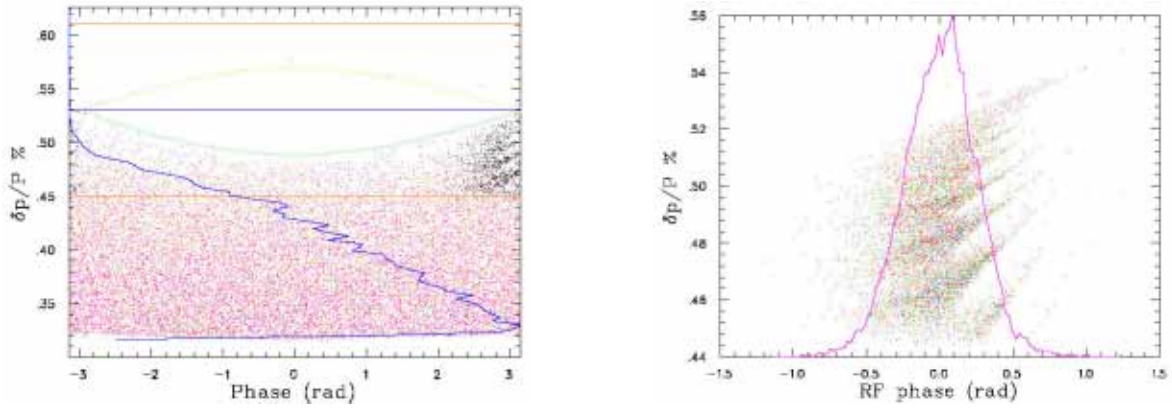


Figure 17: phase space (700ms) and micro-bunch, 03may, $\Delta p/p\% = 0.53$; $\sigma_\phi = 0.42$ ns

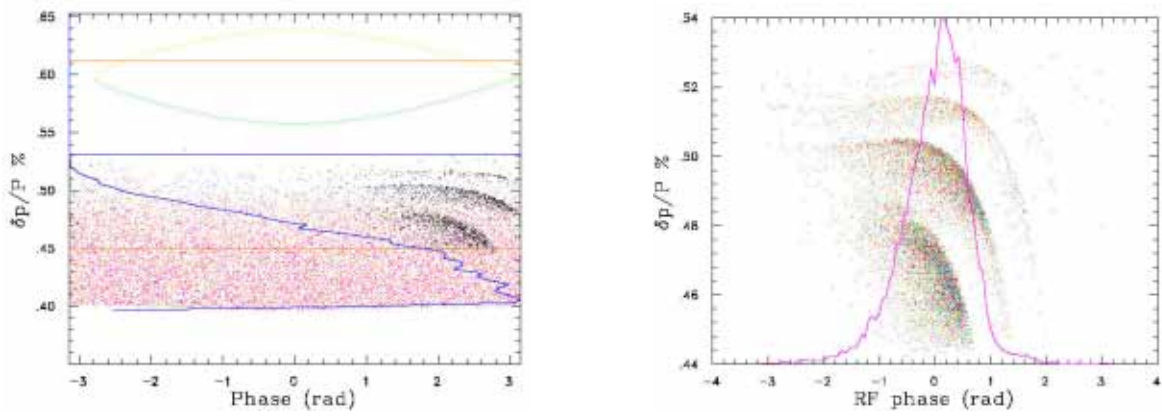


Figure 18: phase space (1100ms) and micro-bunch, 06may, $\Delta p/p\% = 0.60$; $\sigma_\phi = 1$ ns

8.6 may22,18,21,23,16,24,19,17; $\xi = -15.7$, **93 MHz**, $\varepsilon_H = 10\pi\mu\text{m}$

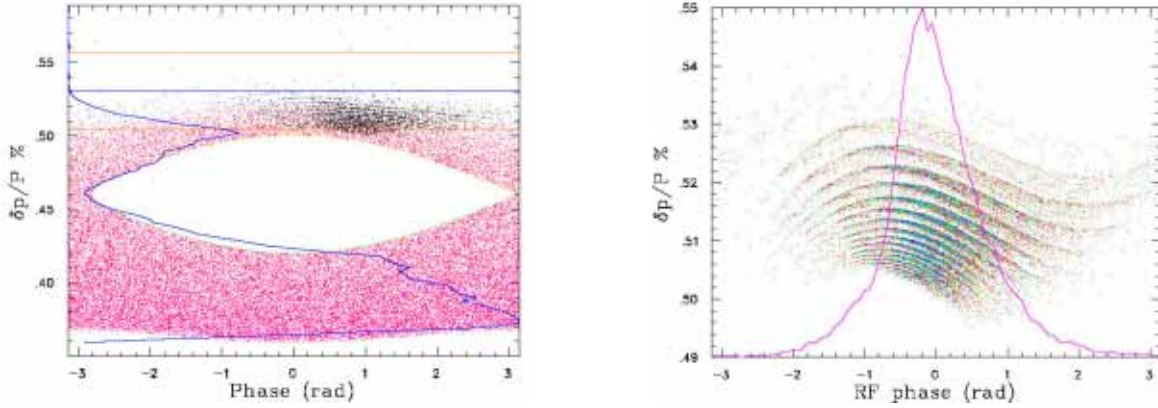


Figure 19: phase space (500ms) and micro-bunch, 22may, $\Delta p/p\% = 0.46$; $\sigma_\phi = 1.24$ ns

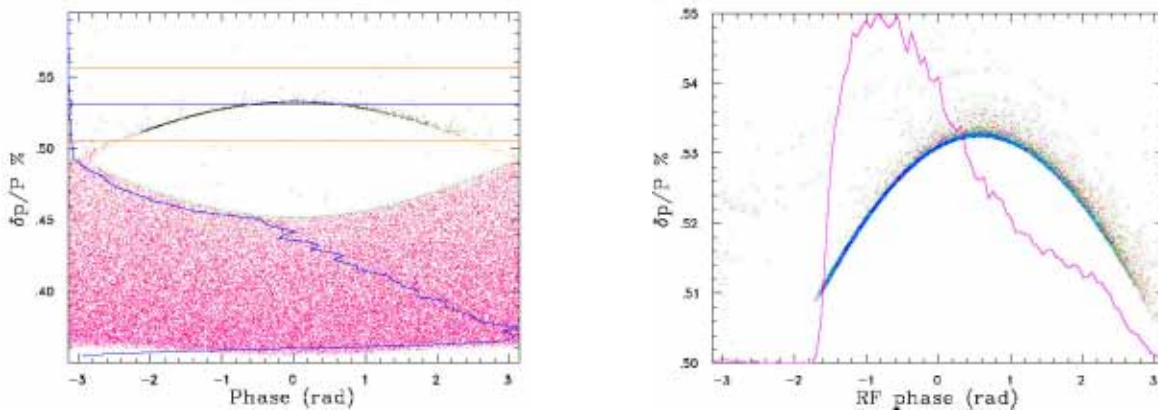


Figure 20: phase space (300ms) and micro-bunch, 18may, $\Delta p/p\% = 0.49$; $\sigma_\phi = 1.8$ ns

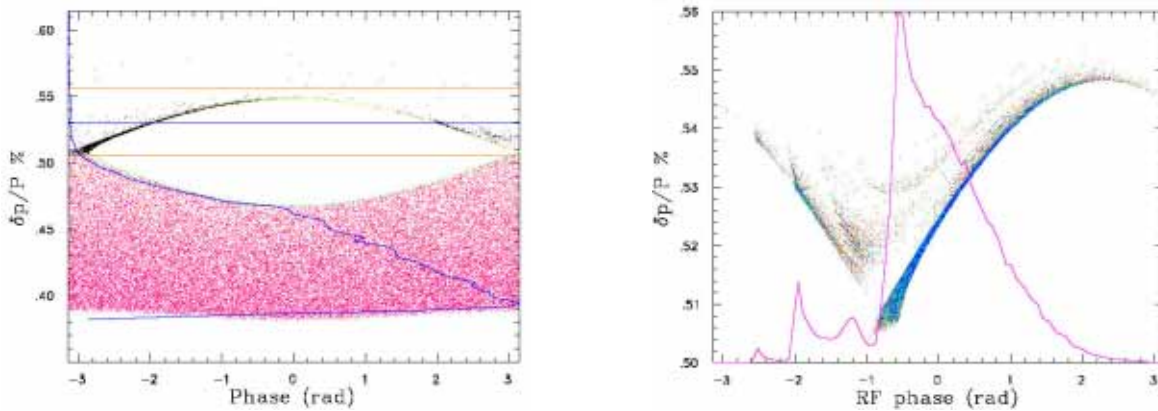


Figure 21: phase space (400ms) and micro-bunch, 21may, $\Delta p/p\% = 0.51$; $\sigma_\phi = 1.4$ ns

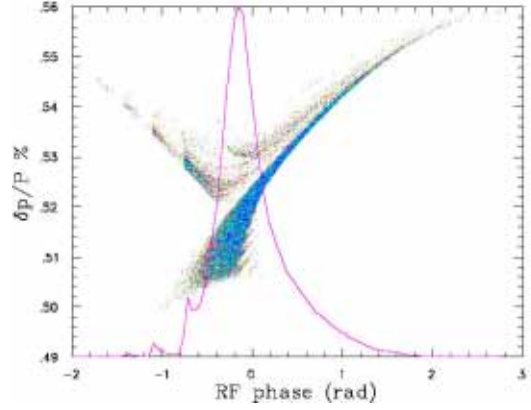
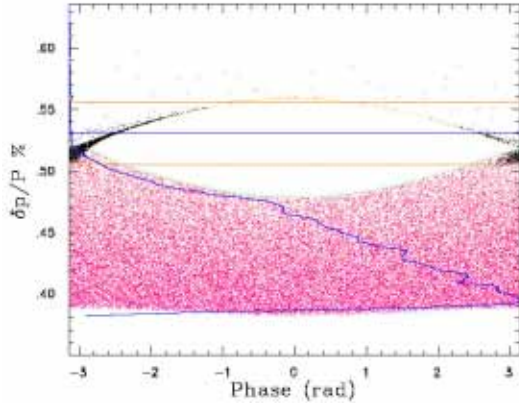


Figure 22: phase space (400ms) and micro-bunch, 23may, $\Delta p/p\% = 0.52$; $\sigma_\phi = 0.74$ ns

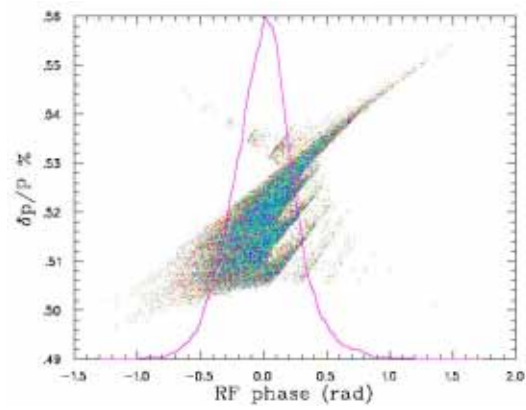
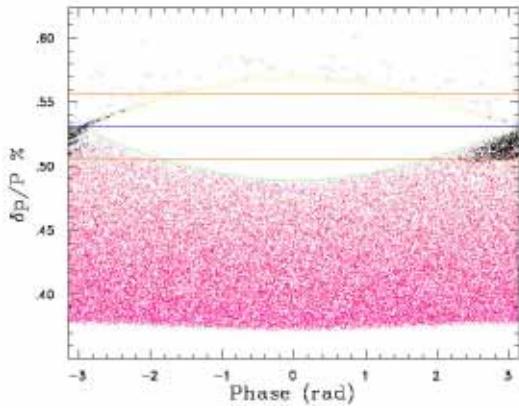


Figure 23: phase space (300ms) and micro-bunch, 16may, $\Delta p/p\% = 0.53$; $\sigma_\phi = 0.44$ ns

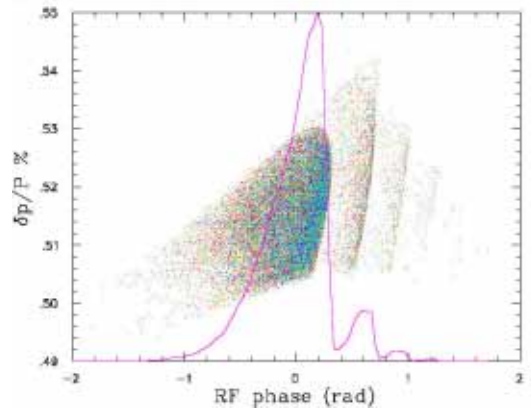
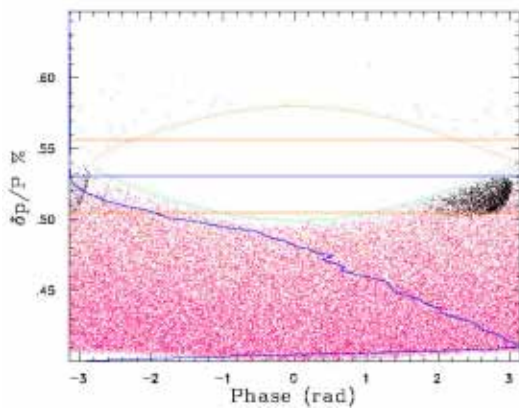


Figure 24: phase space (400ms) and micro-bunch, 24may, $\Delta p/p\% = 0.54$; $\sigma_\phi = 0.55$ ns

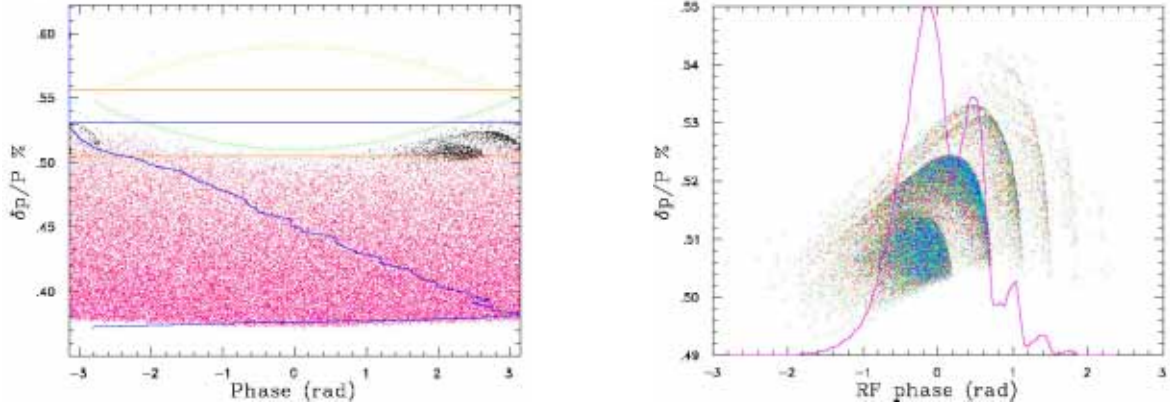


Figure 25: phase space (300ms) and micro-bunch, 19may, $\Delta p/p\% = 0.55$; $\sigma_\phi = 0.89$ ns

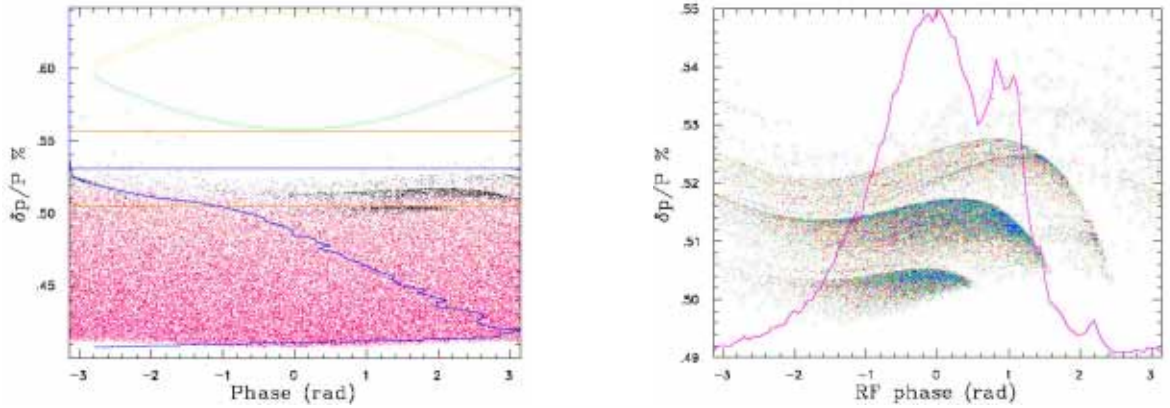


Figure 26: phase space (400ms) and micro-bunch, 17may, $\Delta p/p\% = 0.60$; $\sigma_\phi = 1.69$ ns

9 Output from SLEXPLOT

The following three figures 27,28,29 show example output from SLEXPLOT for case named *25apr* which utilizes dual harmonic for a beam with 95% normalized emittance = 100π μrad . The fundamental has harmonic number 67 which corresponds to a radio-frequency of approximately 25 MHz.

The three figures 30,31,32 show example output from SLEXPLOT for the case named *26apr* which uses a single harmonic voltage waveform for a beam with 95% normalized emittance = 10π μrad . The fundamental (i.e. V_4) has harmonic number 251 which corresponds to approximately 93 MHz.

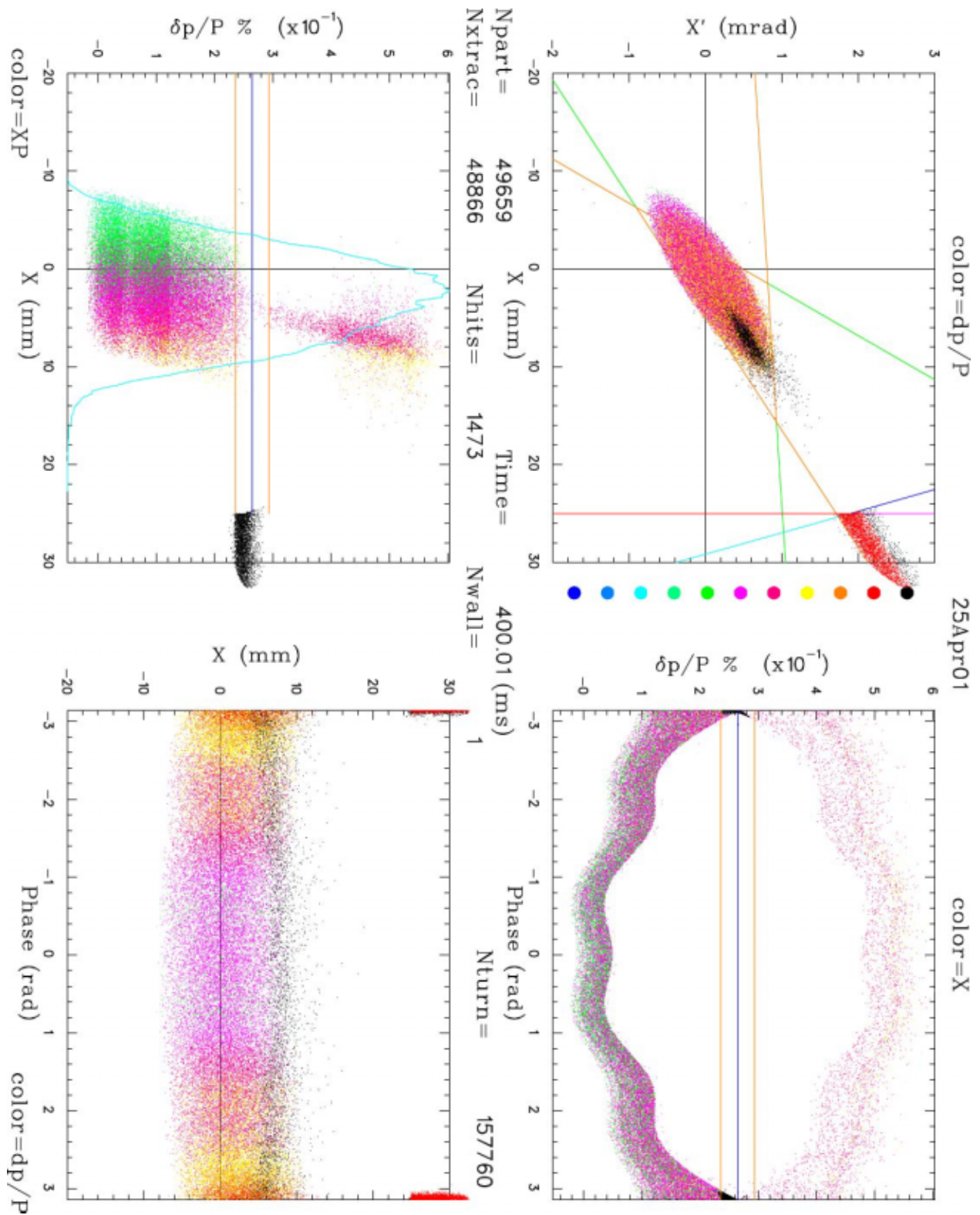


Figure 27: Output from SLEXPLOT option G: General snap-shot of four phase space projections at 400 ms after start of extraction.

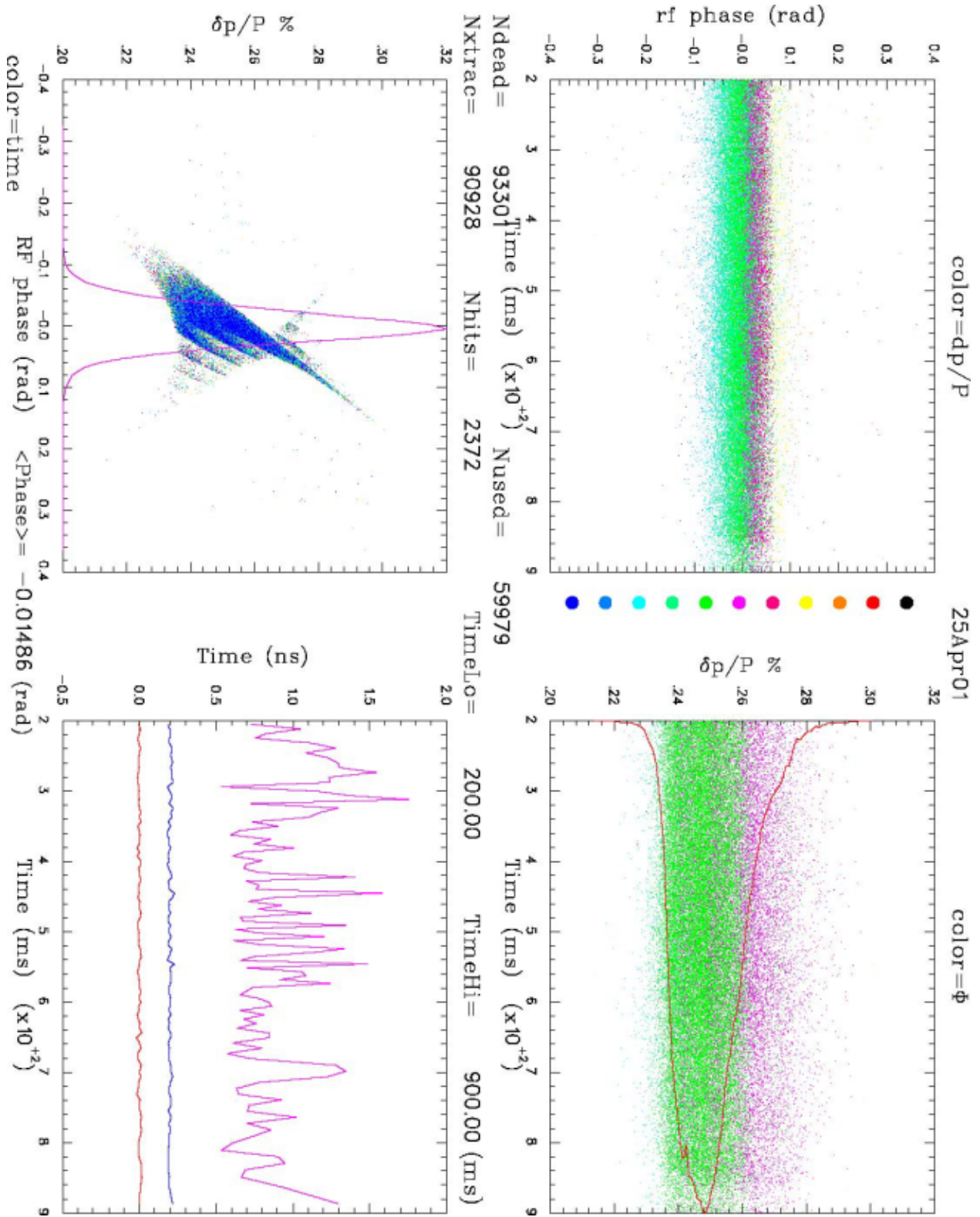


Figure 28: Output from SLEXPLOT option L: Longitudinal properties of extracted beam versus time and $\phi, \delta p$ phase space integrated over the time interval.

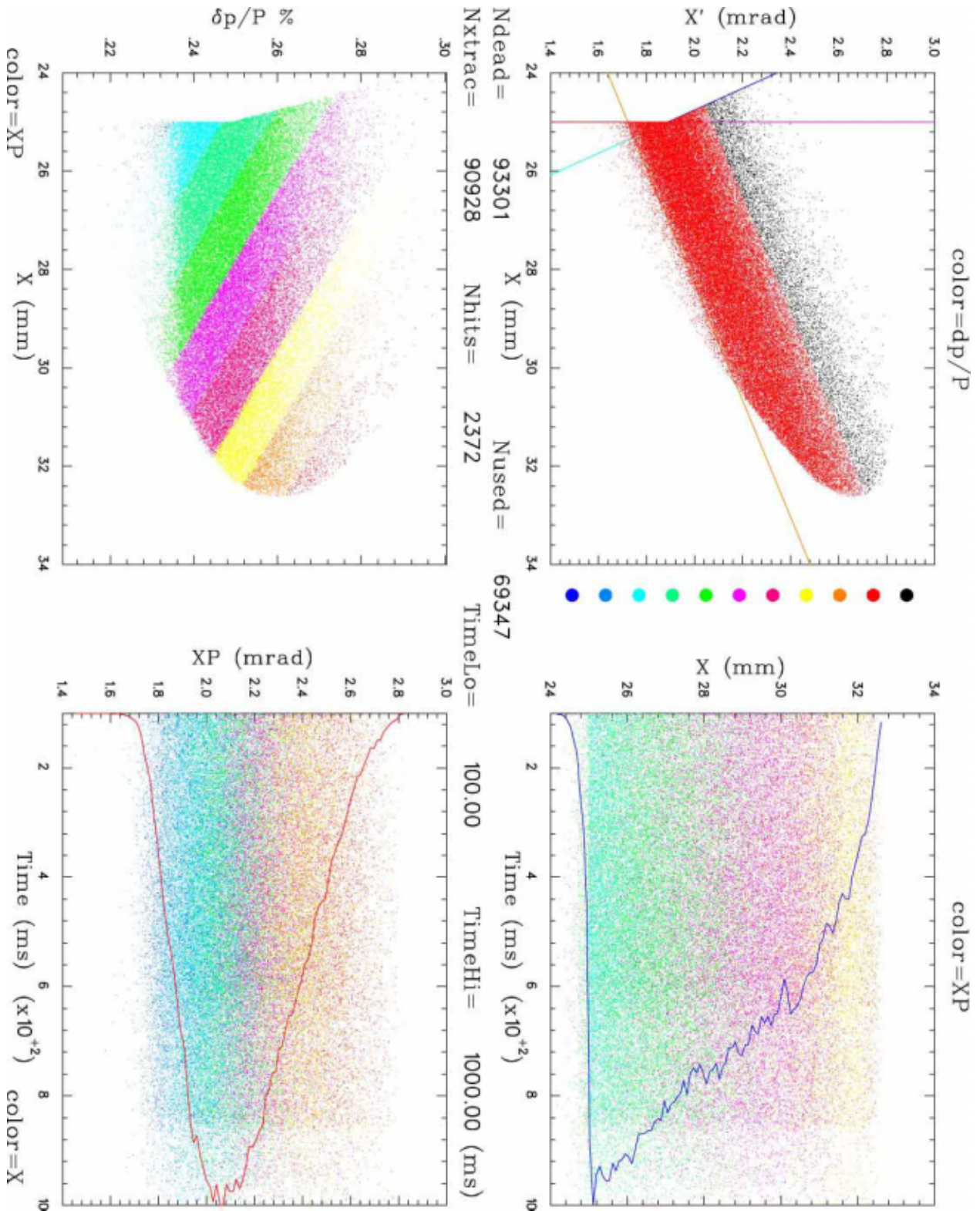


Figure 29: Output from SLEXPLOTT option T: Transverse properties of extracted beam versus time and x, x' phase space integrated over the time interval.

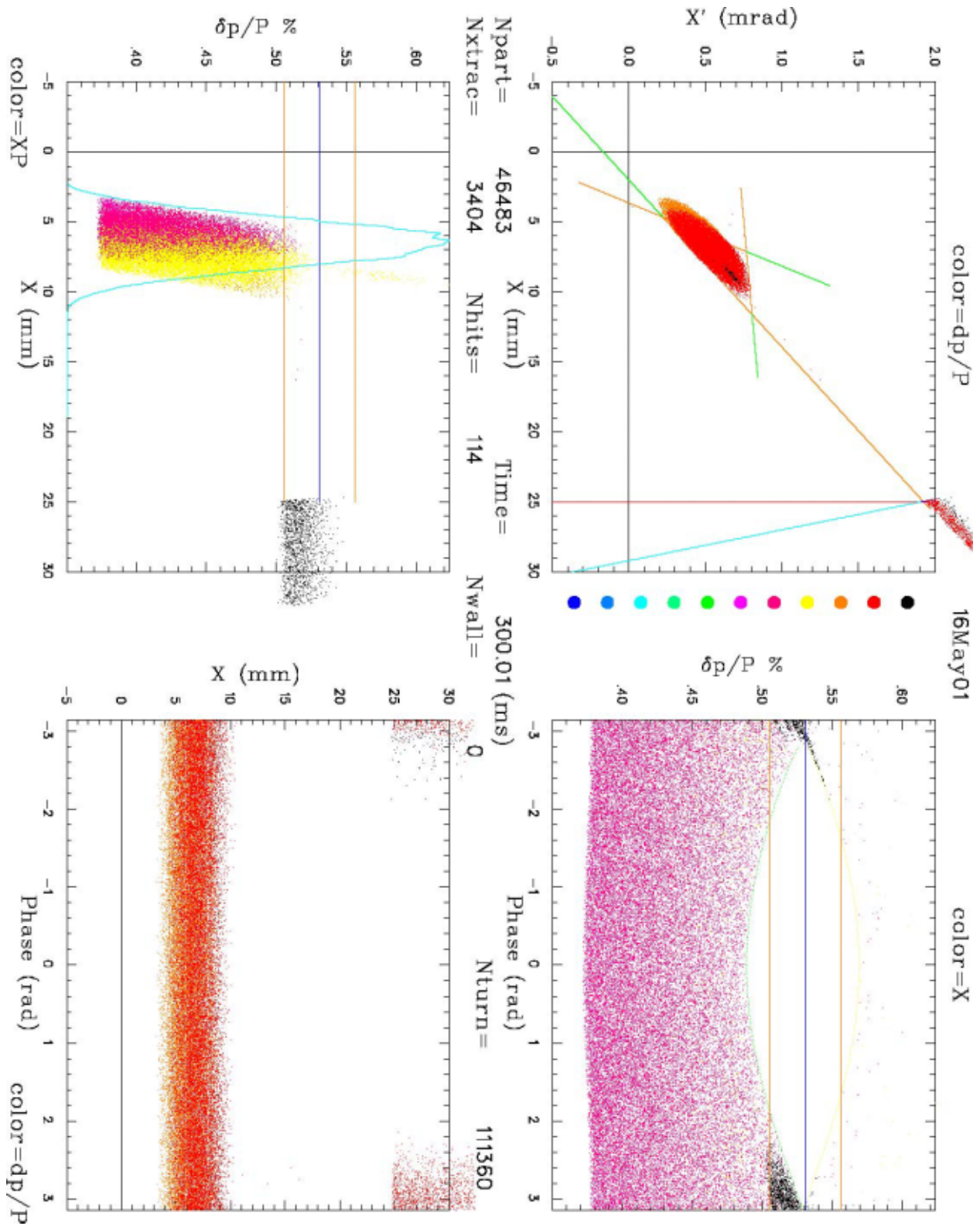


Figure 30: Output from SLEXPLOT option G: General snap-shot of four phase space projections at 300 ms after start of extraction.

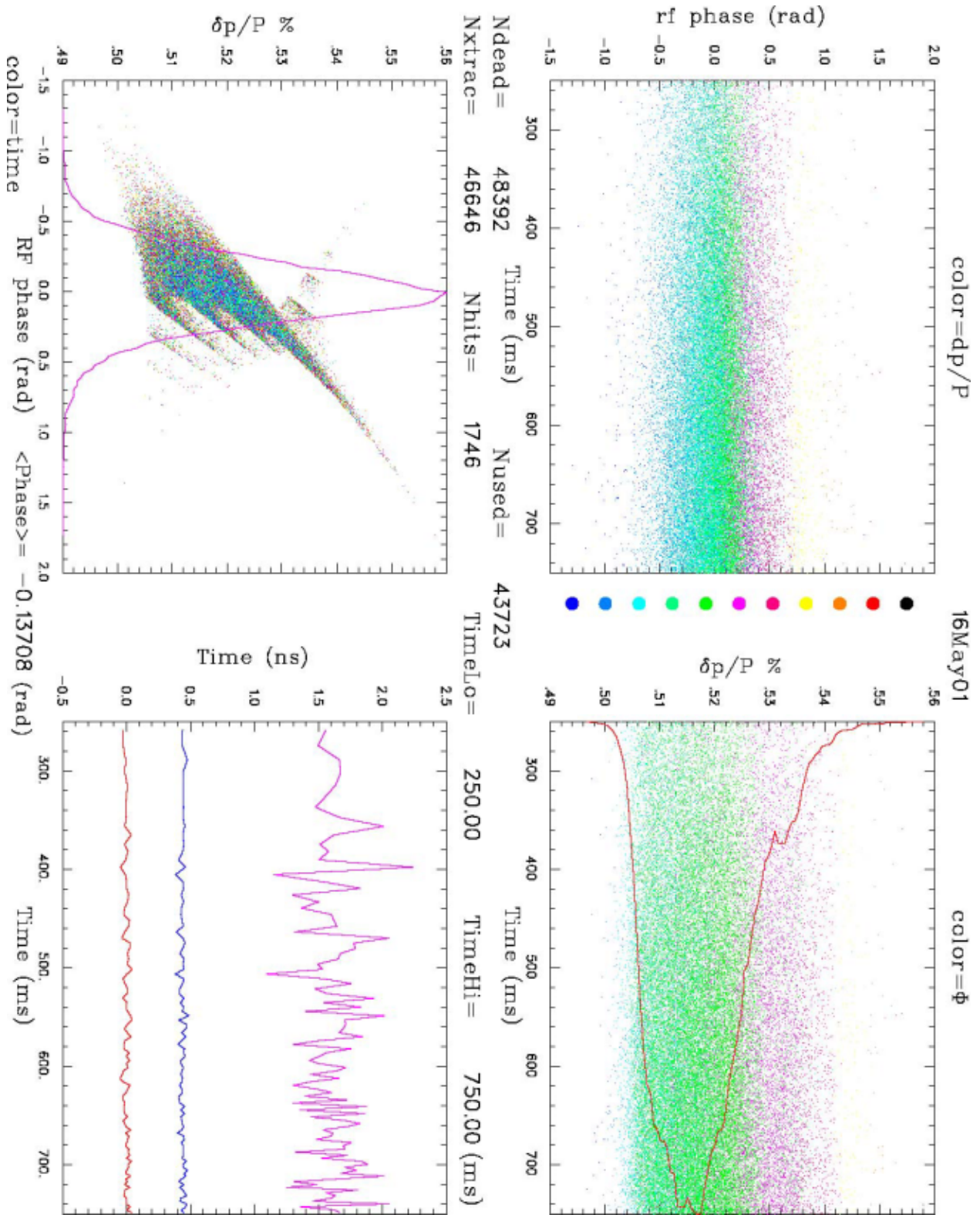


Figure 31: Output from SLEXPLOT option L: Longitudinal properties of extracted beam versus time and $\phi, \delta p$ phase space integrated over the time interval.

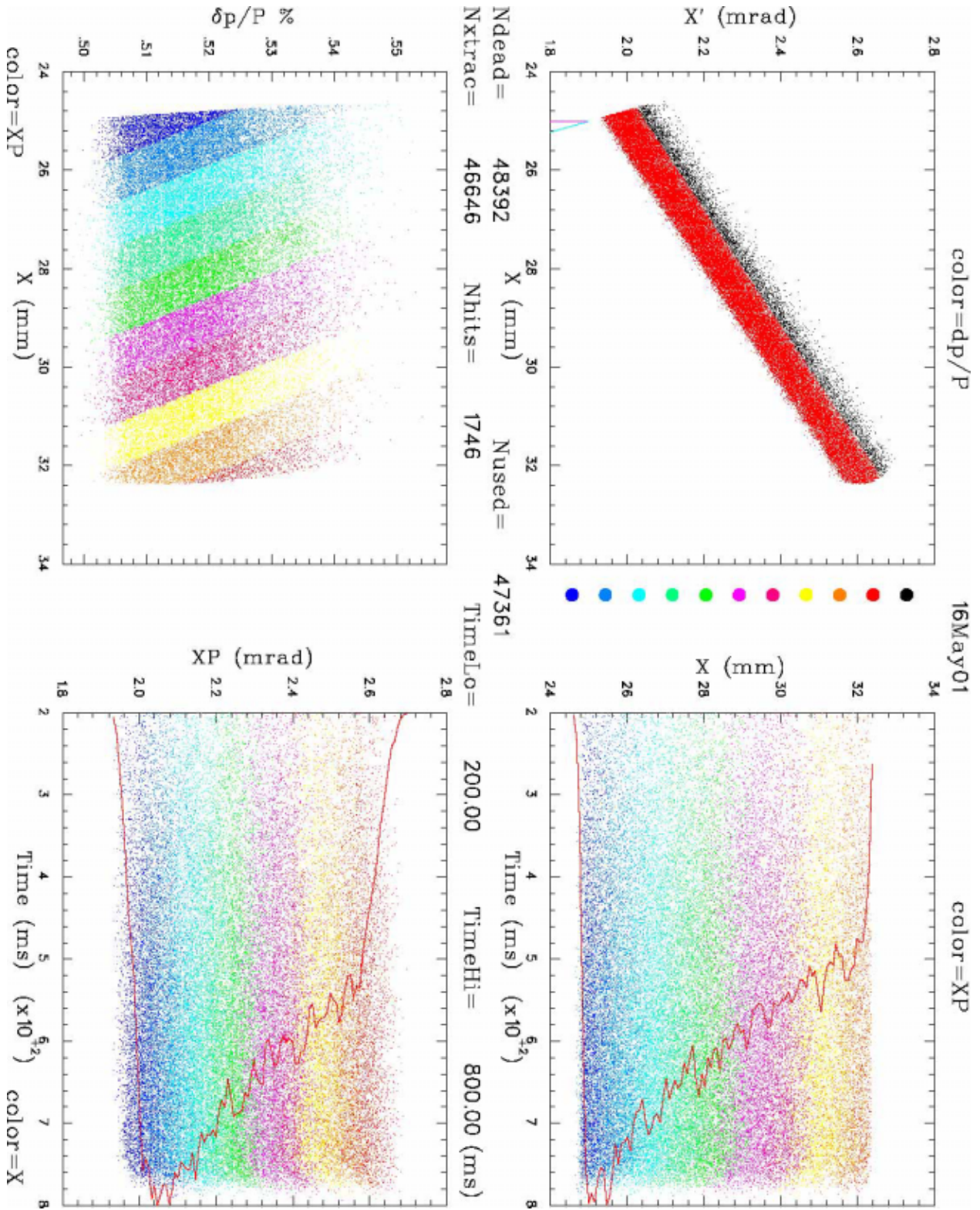


Figure 32: Output from SLEXPLOT option T: Transverse properties of extracted beam versus time and x, x' phase space integrated over the time interval.

10 Tables

10.1 Explanation of symbols

$-\xi$ (#) Machine chromaticity according to the convention $\Delta\nu = \xi\Delta p/p_0$. The natural chromaticity of the AGS is ≈ -31 whereas the partially corrected value is ≈ -16 .

V_n (kV) Voltage of r.f. waveforms.

h (#) Relative harmonic number of the second r.f. component.

$\Delta p/p$ (%) Offset of the momentum centre of the r.f. bucket with respect to the synchronous value dictated by the magnetic field.

A ($\times 10^{-3}$) Normalized sextapole strength.

df/dt (kHz/s) Initial sweep rate of the r.f. buckets into the coasting beam. This non-adiabatic sweep lasts typically 25-50 milliseconds; after which time the radio-frequency slews much more slowly to follow the main bending field.

$\delta p/p$ (10^{-4}) Relative momentum width (dimensionless) containing 66 percent of the particles in the extracted micro-bunch.

σ_ϕ (ns) The root mean square of the bunch time extent $\sigma_\phi = \langle(\phi - \bar{\phi})^2\rangle^{1/2}$ where the mean value is $\bar{\phi} = \langle\phi\rangle$.

66% (ns) The width in nano-seconds containing 66 percent of the particles in the micro-bunch. This width is roughly twice the r.m.s. value σ_ϕ and extends approximately over the range $[-\sigma_\phi, +\sigma_\phi]$ about the mean.

hits (%) The percentage of particles which are extracted from the circulating beam which hit the septum; the sum of head-on and glancing blows. The “hits” represents an inefficiency.

cross (%) The percentage of particles which cross the resonance without being extracted.

$\phi_{a.c.}$ (deg) Phase angle of the fundamental Fourier component of the microbunches.

10.2 Summary of results; 25MHz

Case name	$-B \times 10^3$ (T/s)	$-\xi$ #	V_1 (kV)	V_h (kV)	h #	$\Delta p/p$ %	A 10^{-3}	df/dt kHz/s	$\delta p/p$ 10^{-4}	σ_ϕ (ns)	50% (ns)	66% (ns)	90% (ns)	95% (ns)	99% (ns)	hits %	cross %	$\bar{\phi}_{ac}$ (deg)	Fig. #
05apr	7.727	15.7	100	–	–	0.46	1.0	8.83	4.41	2.97	2.77	4.26	10.7	14.2	17.	8.1	1.01	32.3	4
06apr	7.727	15.7	100	–	–	0.53	1.0	32.	3.45	0.67	0.97	1.35	2.16	2.65	3.60	2.9	1.70	3.96	5
08apr	7.727	15.7	100	–	–	0.598	1.0	11.	2.86	1.36	1.76	2.52	4.67	5.82	8.44	4.5	0.187	-7.91	6
09apr	2.576	15.7	100	100	4	0.53	1.0	32.	3.24	0.371	0.468	0.67	1.20	1.47	2.12	5.6	2.97	-2.24	–
10apr	2.576	15.7	150	150	4	0.53	1.2	32.	3.80	0.371	0.474	0.67	1.19	1.47	2.12	1.8	3.64	-2.65	9
15may	2.576	15.7	150	150	2	0.53	1.4	12.8	4.47	0.391	0.488	0.704	1.28	1.57	2.23	1.2	1.66	-3.20	–
25may	2.576	15.7	150	150	4	0.460	1.25	50.	6.44	1.40	2.32	3.16	5.21	6.05	7.7	4.1	0.7	11.1	7
26may	2.576	15.7	150	150	4	0.495	1.25	44.	6.00	0.669	0.570	0.919	2.47	3.24	4.63	3.0	0.9	2.93	8
28may	2.576	15.7	150	150	4	.5635	1.25	22	3.43	0.637	0.848	1.27	2.05	2.728	3.77	1.2	0.76	-6.13	10
11apr	2.576	15.7	150	150	4	0.598	1.3	33.	3.64	0.743	0.715	1.18	2.61	3.34	4.63	1.0	0.219	-7.47	11
12apr	2.576	15.7	150	–	–	0.598	1.4	33.	3.87	1.03	1.32	1.82	3.25	4.14	6.09	1.1	0.050	-11.0	–
17apr	2.576	15.7	150	150	6	0.598	1.4	33.	5.26	0.80	0.956	1.38	2.67	3.28	4.61	1.2	0.196	-7.97	–
18apr	2.576	15.7	300	–	–	0.598	1.4	33.	5.86	0.99	1.24	1.866	3.21	4.22	5.95	1.2	0.224	-10.24	–
30may	1.288	31.5	150	150	4	0.230	1.0	10.1	2.95	0.771	0.769	1.36	2.80	3.217	4.14	5.1	7?	5.30	12
01jun	1.288	31.5	150	150	4	0.230	1.0	12.6	2.94	0.775	0.761	1.334	2.87	3.26	4.19	5.2	7?	5.29	–
25apr	1.288	31.5	150	150	4	0.264	1.0	28.	1.79	0.200	0.245	0.355	0.646	0.80	1.15	4.1	7.0?	-0.85	13
25ap2	1.288	31.5	150	150	4	0.264	1.0	11.4	1.81	0.214	0.243	0.358	0.663	0.82	1.23	2.9	8.0?	-0.88	–
26apr	1.288	31.5	150	150	6	0.264	1.0	11.4	1.82	0.193	0.240	0.345	0.617	0.768	1.11	3.2	9.0?	-0.908	–
23apr	1.288	31.5	150	150	4	0.299	1.0	23.	1.63	0.438	0.558	0.855	1.59	1.94	2.59	1.5	1.8?	-3.37	14
29apr	1.288	31.5	150	300	4	0.264	1.0	11.4	2.07	0.188	0.231	0.322	0.580	0.716	1.04	2.8	13.6	-0.874	–
30apr	1.288	31.5	150	300	4	0.299	1.0	7.4	1.58	0.363	0.404	0.644	1.29	1.55	2.18	1.9	4.24	-2.92	–

$\varepsilon_H = 100 \pi$.mm.mrad.

10.3 Summary of results; 93MHz

Case name	$-B \times 10^3$ (T/s)	$-\xi$ #	V_4 (kV)	ε_H $\pi \mu\text{mr}$	$\Delta p/p$ %	A 10^{-3}	df/dt kHz/s	$\delta p/p$ 10^{-4}	σ_ϕ (ns)	50% (ns)	66% (ns)	90% (ns)	95% (ns)	99% (ns)	hits %	cross %	$\bar{\phi}_{ac}$ (deg)	Fig. #
01may	1.288	31.5	20	100	0.264	1.0	11×4	1.63	0.233	0.301	0.438	0.814	0.992	1.37	1.3	0.848	-6.51	15
04may	1.288	31.5	20	100	0.299	1.0	0.0	1.66	0.618	0.75	1.05	2.03	2.59	3.70	1.0	.001	-28.1	–
02may	1.288	31.5	100	100	0.264	1.0	11×4	1.52	0.196	0.252	0.362	0.637	0.784	1.12	1.2	2.00	-6.62	16
03may	2.576	15.7	20	100	0.53	1.4	0.0	4.10	0.424	0.581	0.827	1.473	1.783	2.46	1.1	.096	-18.5	17
06may	2.576	15.7	20	100	0.598	1.4	0.0	3.95	1.042	1.18	1.725	3.34	4.40	6.78	1.0	.0074	-53.1	18
17may	2.576	15.7	20	10	0.598	1.4	0.0	1.46	1.69	2.28	3.19	5.40	6.8	9.4	2.9	0.268	-77.8	26
19may	2.576	15.7	20	10	0.550	1.4	0.0	2.00	0.89	1.18	1.77	2.90	3.76	5.10	3.2	0.79	-37.8	25
24may	2.576	15.7	20	10	0.540	1.4	0.0	1.38	0.549	0.70	1.14	2.14	2.62	3.64	3.2	1.5	-23.9	24
16may	2.576	15.7	20	10	0.53	1.4	0.0	1.54	0.438	0.530	0.768	1.423	1.76	2.57	3.6	3.4	-7.88	23
23may	2.576	15.7	20	10	0.518	1.4	0.0	1.95	0.740	0.70	1.12	2.66	3.50	5.14	4.1	1.17	15.1	22
21may	2.576	15.7	20	10	0.508	1.4	0.0	2.49	1.395	2.20	3.29	5.51	6.60	8.60	4.6	0.6	48.7	21
18may	2.576	15.7	20	10	0.492	1.4	0.0	1.79	1.848	2.30	3.86	6.1	7.4	8.0	8.9	0.305	137.	20
22may	2.576	15.7	20	10	0.460	1.4	0.0	1.26	1.24	1.35	2.07	4.23	5.36	7.44	2.9	0.258	-125.	19